Journal of Paleontology

cambridge.org/jpa

Fossil abalones of Europe and their relationships with modern *Haliotis* (Haliotidae, Gastropoda): a multivariate analysis

Stefano Dominici[1,+], Maurizio Forli[2,+], Mauro M. Brunetti[3] and Marco Taviani[4,5]

[1]Museo di Storia Naturale, Università degli Studi di Firenze, Via La Pira 4, I-50121 Firenze, Italy
[2]Via Grocco 16, 59100 Prato, Italy
[3]Calle Navas 106, 14511 Navas del Selpillar, Spain
[4]CNR-ISMAR, via Gobetti 101, 40129 Bologna, Italy
[5]Stazione Zoologica 'Anton Dohrn,' Villa Comunale, 80121 Napoli, Italy

Article

[+]These authors share first authorship

Handling Editor: Olev Vinn

Cite this article: Dominici S, Forli M, Brunetti MM, Taviani M (2025). Fossil abalones of Europe and their relationships with modern *Haliotis* (Haliotidae, Gastropoda): a multivariate analysis. *Journal of Paleontology* 1–32. https://doi.org/10.1017/jpa.2024.50

Received: 29 September 2023
Revised: 22 July 2024
Accepted: 24 July 2024

Corresponding author:
Stefano Dominici;
Email: stefano.dominici@unifi.it

Abstract

Haliotis Linnaeus, 1758, a commercially important gastropod, is the only known genus in the family Haliotidae (Mollusca, Vetigastropoda, or abalone) worldwide. Its poor Cenozoic record and high intraspecific variability resulted in different interpretations of nomenclature, impeding a robust species-level taxonomy and biogeographic history. Among the best-studied forms, three subspecies of *H. tuberculata* Linnaeus, 1758 currently inhabit the temperate waters of the Mediterranean and the eastern Atlantic. New findings in the Pliocene of Tuscany (Italy) are presented here, and the taxonomy of the European record is revised. On the basis of a multivariate analysis of shell morphometrics for the first time applied to the study of fossil abalones, and consistent with the chronostratigraphic and geographic framework, *H. plioetrusca* n. sp. is introduced and *H. volhynica* Eichwald, 1829 and *H. lamellosoides* Sacco, 1897 are reinstated as valid species. Some recently described forms from the Pliocene of Spain are placed in synonymy with *H. lamellosoides*. *Haliotis ovata* Michelotti, 1847 is proposed as the ancestral taxon of modern *H. tuberculata*, via *H. lamellosoides*. This lineage diversified in the subtropical/warm temperate Pliocene Mediterranean, represented by *H. lamellosoides*, *H. bertinii* Forli et al., 2003 and *H. plioetrusca*. The progressive global cooling starting at around 3.0 Ma is associated with the appearance of *H. tuberculata* at temperate latitudes. *H. plioetrusca* is not known from younger strata, whereas *H. bertinii* survived into the Calabrian.

UUID: http://zoobank.org/7c2f2258-2574-4976-a2f5-804c54c86679

Non-technical Summary

The geologic history of abalones, commercially important mollusks living on rocky shores and threatened by overfishing and climate change, is uclear due to a globally poor fossil record and an uncertain taxonomy. Fossils 3.5 million years old found at an exceptionally rich site in Italy are presented, and the European fossil record of abalones is revisited using a quantitative approach to morphological characters. A new Pliocene species is described, and the history of Mediterranean and eastern Atlantic abalones and their evolutionary relationships during the past 23 million years is tentatively reconstructed.

Introduction

The family Haliotidae Rafinesque, 1815 (Mollusca, Vetigastropoda), or abalone, includes 56 extant species and 18 subspecies within the genus *Haliotis* Linnaeus, 1758, distributed in fully marine environments at tropical and temperate latitudes, and many fossil species, often of uncertain status (Geiger, 1998, 2000; Geiger and Groves, 1999; Geiger and Owen, 2012). Abalones are grazing sea snails that commonly inhabit hard substrata at depths of 0–30 m (Geiger and Owen, 2012). Adults feed mostly on drift macroalgae, outcompeting sea urchins within the same guild of macroherbivores when food is not limiting (Jenkins, 2004). They produce an aragonitic shell, with a size up to 120 mm in warm tropical waters (Geiger and Owen, 2012), more than doubling in temperate waters, where *H. rufescens* Swainson, 1822 reaches 313 mm in offshore Oregon (Estes et al., 2005), confirming a latitude–size relationship encountered in other large gastropods (Dominici et al., 2020). The large size of abalones has turned out to be a threat to the survival of natural populations because this shellfish is an important seafood item that has sustained historical commercial fisheries around the world. Overfishing, disease, ocean warming, and acidification recently led to stock collapse, and a few species are now threatened (Rogers-Bennet et al., 2002;

Neuman et al., 2010; Kiyomoto et al., 2013; Li et al., 2018; Rogers-Bennet and Catton, 2019; Wells et al., 2023), including the European green ormer, *H. tuberculata* (Peters, 2021).

The roots of *Haliotis* modern diversity are not simple to trace. Its phylogenetic position within the basal clade Vetigastropoda is unclear (Bouchet et al., 2017), notwithstanding recent efforts based on a comprehensive phylogenomic framework (Cunha and Giribet, 2019). According to the latter, abalones are not closely related to any of the other Vetigastropoda superfamilies, justifying the elevation of the superfamily Haliotoidea to the status of order Haliotida Rafinesque, 1815 (Cunha et al., 2021). If abalones are the sister taxon to the Seguenziida, as still maintained by some (Uribe et al., 2022), then their origin could date back to the Paleozoic. The oldest reported *Haliotis* is found in the Campanian and Maastrichian of California and the Caribbean (Upper Cretaceous; Sohl, 1992; Groves and Alderson, 2008). There are 42 recognized species of *Haliotis*, 38 of which are of Neogene age (<23 Ma; Geiger and Groves, 1999; Estes et al., 2005). Molecular phylogenetic analyses and chromosome evidence suggest that the modern abalone biodiversity hotspot, centered in the tropical Indo-Pacific (Geiger, 2000), originated from a Tethyan ancestor (Geiger and Groves, 1999; Estes et al., 2005; Bester-van der Merwe et al., 2012), a hypothesis consistent with known global dynamics of molluscan diversity (Yasuhara et al., 2022).

The reasons for a poor and confused fossil record are varied. The habitat of abalones is not particularly conducive to preservation of the shell after death (negative taphonomic bias; Geiger and Groves, 1999). Shallow-water rocky substrates are of limited extension and unfavorable to fossilization because of intense hydrodynamic processes that hinder sedimentation and burial and facilitate shell breakage, in addition to mollusk predators (Zuschin et al., 2003; Albano et al., 2022), which include for abalones a variety of bony fishes, crabs, and cephalopods (Geiger and Owen, 2012; Aspe et al., 2019; see also Ponder and Lindberg, 2008). Lower sedimentation rates lead to long exposure to sea water, promoting colonization of the shell by microboring organisms and aragonite dissolution, other important factors of shell loss (Cherns et al., 2011).

The heterogeneity of microhabitats exploited by abalones adds to morphological plasticity of the shell, hinders species recognition, and facilitates taxonomic oversplitting, examples including past and present Mediterranean forms (see for example *H. mykonosensis* Owen, Hanavan, and Hall, 2001; Chiappa et al. 2022). With the preceding limitation in mind, the present paper presents new findings and a revision of the European record of *Haliotis* to shed further light on its geological history on the basis of a large dataset of fossil and Recent shells.

The Upper Cretaceous record from Europe, based on *H. antiqua* Binkhorst, 1861 and *H. cretacea* Lundgren, 1894, has been dismissed due to misidentification (Kaunhowen, 1897; Davies and Eames, 1971). Although very sparse compared with that of other gastropod families, the European record ranges in age from the early Miocene to the Pleistocene (Eichwald, 1829; Hörnes, 1856; Cossmann, 1896; Delhaes, 1909 [fide Geiger and Groves, 1999]; Cossmann and Peyrot, 1917; Glibert, 1949; Baluk, 1975; Krach, 1981; Strausz, 1966; Lozouet et al., 2001b; Forli et al., 2003; Saint Martin et al., 2007; Górka et al., 2012; Forli et al., 2015; Owen and Berschauer, 2017). New species recently described for the Spanish Pliocene are *H. quinquecentenaris* Lozano-Francisco and Vera-Peláez, 2002, *H. iberica* Landau et al., 2003, and *H. telescopica* Vera-Peláez in Vera-Paláez and Lozano-Francisco, 2022. Outside Europe, the fossil record of Haliotidae is much poorer (Geiger and Groves, 1999).

Abalones have a low diversity in the Neogene of Italy. For a long time, Pliocene reports amounted only to *H. lamellosoides* Sacco, 1897 (often under the name *H. tuberculata tuberculata* Linnaeus, 1758), with the relatively recent addition of *H. bertinii* Forli et al., 2003. This paper reports on new findings from southern Tuscany, which allow a significant increase in the understanding of taxonomy and biogeography of Cenozoic to Recent Haliotidae. This report includes a large number of specimens, ranging from juveniles to fully adult shells, found in two outcrops in an area informally known as "Terre Rosse" (meaning "red lands").

Available reviews of the European fossil record attributed most Neogene reports to the living *H. tuberculata* (Geiger and Groves, 1999; Estes et al., 2005), other recently described species mentioned only in passing (Geiger and Owen, 2012). All Oligocene to Pliocene abalones have been grouped under the subspecies *H. tuberculata volhynica*, justified by the extreme plasticity in shell morphology of Atlantic and Mediterranean Recent populations (Geiger and Groves, 1999, p. 872, following Strausz, 1966).

The reappraisal of *H. volhynica* Eichwald, 1829 (Forli et al., 2015; Owen and Berschauer, 2017) and the new data from Terre Rosse presented here allow us to clearly separate *H. volhynica* from the living *H. tuberculata*. For the first time, a multivariate statistical approach is applied to a large quantitative dataset of fossil and extant abalones, and the results are interpreted in the light of traditional taxonomic practice based on descriptive data. Geological relationships between past and present northwestern African and European abalones are re-evaluated.

Geologic and stratigraphic setting

The geographic name "Terre Rosse" informally refers to a small area near Castelnuovo Berardenga, in the province of Siena (Tuscany, Central Italy). It comprises the two localities Stroncoli, where Pliocene yellow sands with lenses of pebbly sand crop out (Forli et al., 2003), and Campino, characterized by yellow sands (Laghi, 1984; Forli et al., 2004, 2021; Cresti and Forli, 2021) (Fig. 1). The Pliocene of the Siena Basin, up to 600 m thick, is formed mainly by marine strata overlain by regressive sediments deposited during the uplift of southern Tuscany, before Pleistocene subaerial exposure (see "Siena sub-basin" in Martini and Aldinucci, 2017). The Terre Rosse succession belongs to nearshore sands and conglomerates of the San Vivaldo Sands Formation, passing southward (basinward) to offshore muds (informally known as "Blue Clays"; Martini and Aldinucci, 2017). The Stroncoli and Campino shallow-water pebbly and shelly sandstone unit from which abalones were collected is here tentatively referred to the informal chronostratigraphic units S3 and S4 recognized in the nearby Guistrigona area (Martini and Aldinucci, 2017; late Zanclean–early Piacenzian = ca. 4.0–3.0 Ma).

The Terre Rosse abalones were compared with available data from other Italian and European collections (see abbreviations that follow). Stratigraphy and provenance of specimens of the historical collection of Luigi Bellardi and Federico Sacco, collected in northwestern Italy and hosted in the Museum of Natural History of Turin, were taken from Ferrero Mortara et al. (1982). These fossils range in age from the middle Burdigalian (early Miocene, ca. 19.0–17.0; Zunino and Pavia, 2009) to the early

https://doi.org/10.1017/jpa.2024.50 Published online by Cambridge University Press

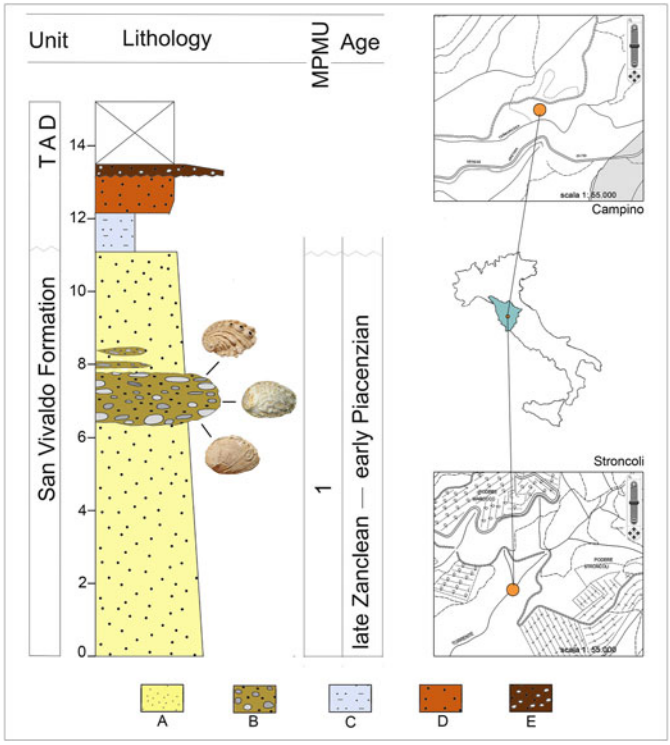

Figure 1. Stratigraphic log of the Pliocene of the Terre Rosse area (Siena basin; late Zanclean–early Piacenzian). TAD = terraced alluvial deposits (Quaternary); A = sands; B = pebbly sands; C = clays; D = silty sands; E = gravels. Top right, locality Campino; bottom right, locality Stroncoli (scale 1:55.000).

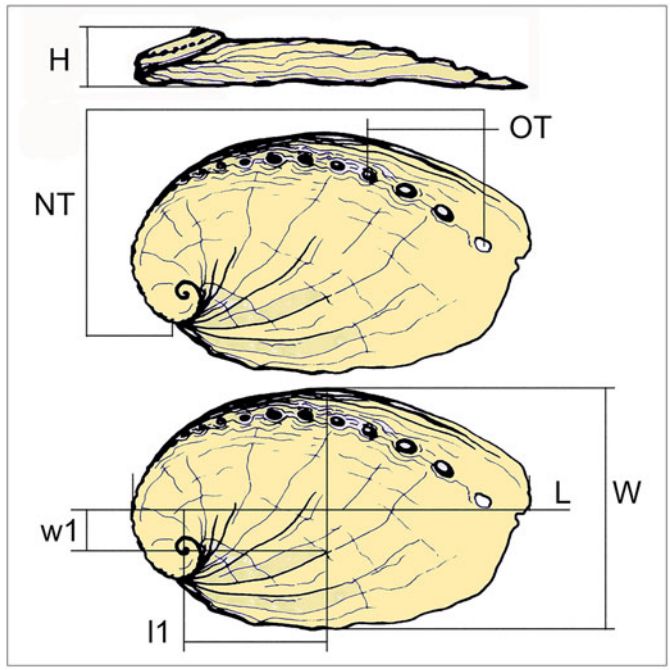

Figure 2. *Haliotis* shell morphometrics: L = maximum length; l1 = length from apex to L midline; W = maximum width; w1 = width from apex to W midline; H = height from apex to aperture; NT = total number of tremata, from the contact of the whorl with the posterior labial margin to the anterior end of the row; OT = open tremata.

Pleistocene (= ca. 2.5–1.0 Ma; Sacco, 1897). Most studied specimens of *H. volhynica* were collected at Maksymivka (Ternopil, Ukraine; see Radwański et al., 2006), in middle Miocene fully marine deposits of eastern Europe that can be correlated with the Serravallian (= 14.0–12.0 Ma; Śliwiński et al., 2012).

Materials and methods

Terre Rosse fossiliferous strata were bulk sampled, and additional shells were surface collected in the field. Specimens were isolated from the residue after wet-sieving sediment through a 1 mm-size screen. Shells (not casts or molds) in public institutions and in private collections, or their photographs in the literature, were measured. The initial dataset included 379 specimens (153 fossil, 226 Recent specimens; Supplementary Material, dataset 1).

Morphological characters useful for the species- and subspecies-level taxonomy of abalones are general shape; position of apex; spire height; position, number, and shape of tremata; axial and spiral ornamentation; shape and position of the columnellar fold; and size (Geiger and Groves, 1999). We measured shell length (L), shell length from apex to L midline (l_1), shell width (W), shell width from apex to W midline (w_1), shell height (H), and number of tremata, separating total number (NT) from open tremata (OT; Fig. 2). Incomplete specimens were discarded, and statistical analysis was performed on 82 fossils and 124 Recent specimens belonging to 15 taxa recognized on traditional descriptive grounds. Secondary data to explore changes in shell shape among these a priori groups included height:length ratio (H/L), width:length ratio (W/L), height:width ratio (H/W), rate of length increase (l_1/L), and rate of width increase (w_1/W).

Extant taxa included in the large dataset (Supplementary Material, dataset 1) are *H. tuberculata tuberculata* Linnaeus, 1758, *H. t. coccinea* Reeve, 1846, *H. t. fernandesi* Owen and Afonso, 2012, *H. stomatiaeformis* Reeve, 1846, *H. tuberculata* "Dakar", *H. geigeri* Owen, 2014, *H. pustulata* Reeve, 1846, and *H. marmorata* Linnaeus, 1758. All specimens for which not all of the morphometrics could be measured (mainly H) were removed, resulting in a first set of specimens upon which to perform a statistical analysis (Supplementary Material, dataset 2).

Fossil taxa are *H. benoisti* Cossmann, 1896, *H. volhynica* Eichwald, 1829, *H. lamellosoides* Sacco, 1897, *H. bertinii* Forli et al., 2003, *H. plioetrusca* n. sp., *H. stalennuyi* Owen and Berschauer, 2017, *H. ovata* Michelotti, 1847, *H. monilifera* Michelotti, 1847, and *H. torrei* Ruggieri, 1990. The last four species, being scantily represented, were excluded from the statistical analysis applied to a third subset (Supplementary Material, dataset 3).

All multivariate analyses were performed using RStudio (version: 2023.12.1+402), with the stats (R Core Team, 2022) and vegan (Oksanen et al., 2022) packages.

Notwithstanding the advantage of exploring potentially covariate morphometrics, multivariate analysis of morphological traits has rarely been applied to the study of abalone shell, only at the population level (McShane et al., 1994; Bachry et al., 2019) and never on fossils. A recent multivariate approach applied to a conchological study of cowries (Southgate and Militz, 2023)—also a group of large gastropods with considerable infraspecific variation in shell form—offered a template for the ordination and statistical study of abalones. On the basis of that experience, non-metric

https://doi.org/10.1017/jpa.2024.50 Published online by Cambridge University Press

multidimensional scaling (nMDS) was preferred to other techniques (e.g., principal component analysis) for resolving group differences when studying general shell form. While cowries have a smooth outer surface, the abalone shell offers characters such as ribs, tubercles, and lamellae as an additional means to diagnose taxa. These last characters were left unquantified but used nonetheless as diagnostic characters to define a priori groups, following traditional taxonomic practice (e.g., Geiger and Owen, 2012; Owen and Berschauer, 2017).

For multivariate analysis, values resulting from both dimensionless and differently scaled measurements were transformed to Z-scores before testing (R function: scale) so that each morphometric was centered, with a mean of zero, and uniformly scaled, with values expressed in terms of deviation from the mean (i.e., |Z-score| > 3). We identified atypical specimens if at least one morphometric exceeded three standard deviations of the mean. A resemblance matrix was computed on the basis of Euclidean distances between the remaining specimens (R function: vegdist) and visualized in two dimensions through nMDS (R function: metaMDS). We measured the coefficient of determination (R^2, or squared correlation) on the basis of morphometric variables and ordination scores (R function: envfit). The results of each morphometric were then overlayed on the existing nMDS ordination and visualized through morphometric clines (R function: ordisurf) to isolate the influence of each morphometric on the plot configuration.

To avoid the subjectivity of visual interpretations of multidimensional data after reducing dimensionality and thereby validate differences in shell form among a priori groups, a one-factor permutational analysis of variance (PERMANOVA) was used to assess whether within-group distances are smaller than among-group distances (R function: adonis2). We used the F-value to measure the ratio of within- and among-species variance in morphospace. Permutation-based tests for homogeneity of multivariate dispersions were used to assess whether dispersions (the distance of specimens from their group centroid) vary among groups (R function: permutest.betadisper; for other details on the multivariate analyses, see Southgate and Militz, 2023; the script adapted to the present dataset is available in the Supplementary Material). Boxplots were used to visualize differences in mean and median tendencies, range, and quantiles of morphometrics among groups.

Biogeographic provinces discussed in the study, following Geiger (2000, p. 58), are Northeast Atlantic (western Atlantic from Normandy, France, to western Morocco, 30°N); Mediterranean (Mediterranean Sea); West African (central and southwestern Atlantic, from 30°N, including Canary Islands, to Cape Town, Republic of South Africa); Red Sea (North of Djibouti).

Most French fossil sites can be located following Lozouet et al. (2001a), to the exclusion of Nouvelle-Aquitaine, Vienne, Moulin Pochard, with coordinates 48.053°N, 0.670°E. Italian sites include Petralia Sottana, Palermo (37.804°N, 14.082°E); Stroncoli, Siena (43.19594°N, 11.35428°E); Campino, Siena (43.20176° N, 11.34463°E); and Quercecchio, Siena (43.030°N, 11.413°. Ukranian sites include Ternopil, Maksymivka quarry (49.361°N, 25.543°E).

Suprageneric systematics follows the World Register of Marine Species (WoRMS, 2023). Abbreviations: H = height from apex to horizontal plane; L = maximum length; l1 = length from apex to L midline; W = maximum width; w1 = width from apex to W midline; NT = total number of tremata from the contact of the whorl with the posterior labial margin to the end of row in anterior part; OT = number of open tremata. Size is expressed in millimeters throughout the paper.

Repositories and institutional abbreviations. Figured specimens and other material examined in this study are deposited in the following institutions: British Museum of Natural History (BMNH), London, United Kingdom; Linnean Society of London (LSL), London, UK; Museo di Storia Naturale, Università di Firenze (MSNF IGF), Firenze, Italy; Museo di Storia Naturale di Milano, (MSNM), Milano, Italy; Museo Regionale di Scienze Naturali (MRSN), Torino, Italy; Museo di Zoologia, Università di Bologna (MZB), Bologna, Italy; National Museum of New Zealand (NMNZ), Wellington, New Zealand; Natuurhistorisch Museum Rotterdam (NHMR), Rotterdam, Netherland; Muséum d'Histoire naturelle de Bordeaux (MHNBx), Bordeaux, France; Muséum national d'Histoire naturelle (MNHN), Paris, France; Wiener Naturhistorische Museum (NHMW), Wien, Austria.

Private collections temporarily hosting specimens are: CLZ, Alain Cluzaud (France); JLC, Jean-François Lesport (France); RMQ, Robert Marquet (Belgium); BDA, Bruno dell'Angelo (Italy); CBC, Cesare Bogi (Italy); FCC, Fabio Ciappelli (Italy); MCC, Massimo Cresti (Italy); MFC, Maurizio Forli (Italy); MRC, Massimo Rocca (Italy); MBB, Mauro M. Brunetti (Spain).

Others collections are: BOC, Buzz Owen, California, USA; DDC, Dwayne Dinucci, California, USA; FFC, Franck Frydman, Paris, France; FRC, Ramiro Fladeiro, Valhascos, Portugal; PRC, Peter Ryall, Austria; RKC, Robert Kershaw, NSW, Australia; (Owen et al., 2015).

Results

Haliotis *at Terre Rosse.—Haliotis lamellosoides* is everywhere abundant in the area (16 specimens at Campino, 79 at Stroncoli), whereas *H. bertinii* (14 specimens) and *Haliotis plioetrusca* n. sp. (13 specimens) were found only at Stroncoli, a site with a total of 106 abalone specimens. The abundant biometric data available for *H. lamellosoides*, including both juvenile and adult individuals, testify to a wide range of variability of this species and suggest including in its synonymy recently described species at Estepona, Spain (Lozano-Francisco and Vera-Peláez, 2002; Landau et al., 2003; Vera-Peláez in Vera-Paláez and Lozano-Francisco, 2022).

The Terre Rosse fossils greatly contributed to the significance of the multivariate analysis of fossil abalone, with 50 out of 76 fossils of the quantitative subset (Supplementary Material, dataset 3).

Multivariate analysis was performed on successive subsets of the whole, until two of them were selected to build meaningful and more easily interpretable matrices. The first set includes Recent specimens of Mediterranean and Atlantic species and subspecies of Europe and northwestern Africa. All specimens of the larger dataset that did not allow us to measure morphometric H were excluded. The a priori groups in this set are *H. stomatiaeformis* Reeve, 1846 (N = 27), *H. tuberculata tuberculata* Linnaeus, 1758 (N = 32), *H. t. coccinea* Reeve, 1846 (N = 29), *H. t. fernandesi* Owen and Afonso, 2012 (N = 4), and a population of *H. tuberculata* from Dakar (Senegal), formerly attributed to *H. speciosa* Reeve, 1846 (N = 20) (Supplementary Material, dataset 2). The first three taxa were recently validated by molecular data (Chiappa et al., 2022) to offer reliable a priori groups to test the multivariate approach.

https://doi.org/10.1017/jpa.2024.50 Published online by Cambridge University Press

The second matrix included species-level data collected from Neogene fossils of Europe and previously recognized by taxonomists. This set includes *H. benoisti* Cossmann, 1896 (N = 11), *H. volhynica* Eichwald, 1829 (N = 11), *H. lamellosoides* (Sacco, 1897) (N = 37), *H. bertinii* Forli et al. 2003 (N = 8), and the Stroncoli paleo-population of *H. plioetrusca* (N = 11). Two further taxa were considered during a preliminary trial, namely *H. ovata* Michelotti, 1847 and *H. torrei* Ruggieri, 1990, but discarded because of insufficient data. All specimens of *H. tuberculata* in the strict sense (excluding subspecies from Macaronesia and Senegal) of the first dataset were included in the second matrix to compare fossil abalones with the two extant European abalones (Chiappa et al., 2022).

The a priori assigned groups of the first dataset (i.e., *H. stomatiaeformis*, *H. tuberculata tuberculata*, *H. t. coccinea*, *H. t. fernandesi*, and the Dakar population of *H. tuberculata*) were capable of explaining a significant amount ($R^2 = 0.42$, $F = 18.762$, $p < 0.0001$) of the variation in shell form (Fig. 3.1). Differences of shell form among species were highly significant judging from F, or the ratio of within- and among-species variance in morphospace (Table 1) and particularly when confronted with molecular data (Chiappa et al., 2022), allowing us to distinguish *H. stomatiaeformis* from *H. tuberculata*, particularly from the other Mediterranean abalone *H. t. tuberculata* ($F = 52.23$, $p = 0.0001$: if *p* is insignificant, then the significant F from PERMANOVA, like in this case, indicates that the differences are driven by differences in centroids). Subspecies *H. t. tuberculata* and *H. t. coccinea* show some overlap ($F = 16.21$, $p = 0.0001$), confirming a limited gene flow suggested by molecular studies (Chiappa et al., 2022). The overlap increases between *H. t. fernandesi* and *H. t. coccinea* ($F = 4.82$, $p = 0.0013$). Shell form for the Dakar population of *H. tuberculata,* formerly attributed to *H. speciosa*, was distinct from *H. stomatiaeformis* ($F = 33.80$, $p = 0.0001$), overlapping with *H. t. coccinea* ($F = 7.37$, $p = 0.0001$) and *H. t. fernandesi* ($F = 4.13$, $p = 0.0035$) and strictly comparable to that of *H. t. tuberculata* ($F = 2.71$, $p = 0.0283$; Fig. 3.1; Table 1).

All morphometrics considered representative of shell form (i.e., L, H/L, W/L, H/W, l_1/L, w_1/W, NT, OT) significantly influenced the ordination structure of the abalone groups visualized in Fig. 3. The most important morphometric was l_1/L ($R^2 = 0.82$, $p < 0.001$), followed by NT ($R^2 = 0.78$, $p < 0.001$), H/W ($R^2 = 0.72$, $p < 0.001$), L ($R^2 = 0.72$, $p < 0.001$), OT ($R^2 = 0.67$, $p < 0.001$), H/L ($R^2 = 0.57$, $p < 0.001$), W/L ($R^2 = 0.31$, $p < 0.001$), and last w_1/W ($R^2 = 0.31$, $p < 0.001$; not shown in Fig. 3). Most univariate methods allow us to separate *H. stomatiaeformis* from *H. tuberculata*, with the exception of w_1/W (Figs 3.2–3.8, 4).

Since the results of the nonmetric MDS of the first dataset are consistent with an approach to the taxonomy of the family that includes genetic data (Chiappa et al., 2022), the same multivariate statistics can be used to separate species known only from fossils, whose taxonomic status relies only on shell morphology. The a priori groups in the second dataset, including both extinct and extant taxa (i.e., *H. benoisti*, *H. lamellosoides*, *H. volhynica*, *H. plioetrusca*, *H. tuberculata*, and *H. stomatiaeformis*), were able to explain a highly significant amount ($R^2 = 0.56$, $F = 25.832$, $p < 0.001$) of the variation in shell form (Fig. 5.1). The multivariate approach was particularly significant (Table 2), with *H. plioetrusca* dissimilar to *H. stomatiaeformis* ($F = 57.03$, $p = 0.0001$), *H. benoisti* ($F = 27.42$, $p = 0.0001$), and *H. volhynica* ($F = 26.20$, $p = 0.0001$), and *H. benoisti* and *H. volhynica* the most similar ($F = 3.63$, $p = 0.0023$; Fig. 5). Similar pairs include *H. tuberculata* and *H. plioetrusca* ($F = 7.92$, $p = 0.0001$) and *H. lamellosoides* and *H. plioetrusca* ($F = 11.38$, $p = 0.0001$). *H. stomatiaeformis* is distinct from *H. benoisti* ($F = 18.56$, $p = 0.0001$) and *H. volhynica* ($F = 20.37$, $p = 0.0001$), and particularly from *H. tuberculata* ($F = 57.16$, $p = 0.0001$). Finally, multivariate analysis separates *H. lamellosoides* from *H. tuberculata* ($F = 20.43$; $p = 0.0001$; Fig. 5.1; Table 2).

Similarly to the results obtained from the first dataset, also working with fossil taxa morphometrics considered representative of shell form significantly influenced the ordination structure (Fig. 5.2–5.8), with some differences in rank. The most important morphometric was NT ($R^2 = 0.81$, $p < 0.001$), followed by H/W ($R^2 = 0.70$, $p < 0.001$), OT ($R^2 = 0.70$, $p < 0.001$), L ($R^2 = 0.70$, $p < 0.001$), W/L ($R^2 = 0.64$, $p < 0.001$), H/L ($R^2 = 0.58$, $p < 0.001$), l_1/L ($R^2 = 0.35$, $p < 0.001$), and w_1/W ($R^2 = 0.12$, $p < 0.001$; not shown in Fig. 5). Univariate analysis expressed through bloxplots (Fig. 6) underline that the relative position of the spire (morphometrics l_1/L and w_1/W) and the number of open tremata (OT) do not allow us to differentiate among abalone species (Fig. 6.5–6.8), whereas all other morphometrics clearly separate Miocene and Pliocene European abalones, with extant *H. stomatiaeformis* being more similar to the first, and *H. t. tuberculata* to the second.

Ultimately, from the associations between each morphometric and nMDS plot configurations (Figs 3.2–3.8, 5.2–5.8), relative differences in shell form could be inferred, analogously to results obtained by applying the same technique to cowries (Southgate and Militz, 2023), confirming the general utility of multivariate morphometric methods for statistical comparison of shell form between gastropod species (and to a lesser extent to subspecies). The two sets shared NT, H/W, OT, and L among the most informative morphometrics.

Systematic paleontology

Family **Haliotidae** Rafinesque, 1815
Genus ***Haliotis*** Linnaeus, 1758

Type species. *Haliotis asinina* Linnaeus, 1758 Recent, Eastern Indian Ocean to the Central Pacific, by subsequent designation Montfort, 1810.

Remarks. The supraspecific taxonomy of haliotids is problematic, and the use of a single genus-level taxon *Haliotis* is warranted (Geiger and Owen, 2012).

Haliotis benoisti Cossmann, 1896
Figures 7, 8.1–8.4

1896 *Haliotis benoisti* Cossmann, p. 22, pl. 5, figs. 14, 15.
1903 *Haliotis neuvillii* Bial de Bellerade, p. 196.
1917 *Haliotis benoisti*; Cossmann and Peyrot, p. 224, pl. 3, figs. 7–9, pl. 10, fig. 36.
1918 *Haliotis benoisti*; Cossmann, p. 314, pl. 10, figs. 38, 39.
1999 *Haliotis tuberculata volhynica* Eichwald; Geiger and Groves, p. 875.
2001b *Haliotis* (*Sulculus*) *benoisti*; Lozouet et al., p. 16, pl. 3, fig. 4.

Type material. Holotype, MNHN. F. J04614, L 4.0 mm (Fig. 8.3–8.4). Paratypes (four specimens): MNHN.F.J04615. Type locality: France, Gironde, Mérignac, Aquitanian Basin, early Miocene, Aquitanian.

Occurrence. France: from late Oligocene to early Miocene (Aquitanian–Burdigalian), Lariey, Léognan, Martillac, Mérignac, Western Atlantic France, Aquitanian Basin.

https://doi.org/10.1017/jpa.2024.50 Published online by Cambridge University Press

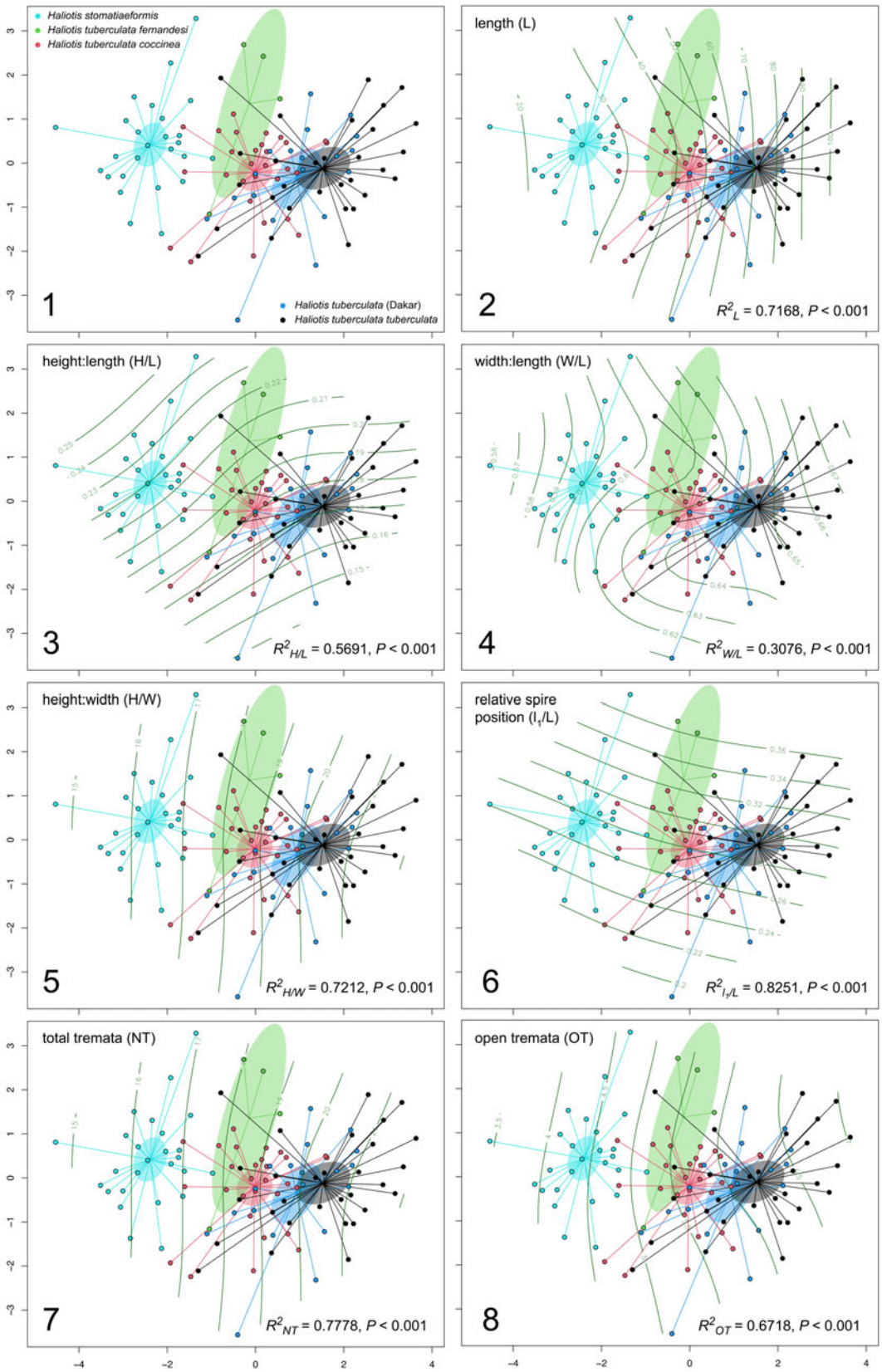

Figure 3. (**1**) nMDS ordination (stress = 0.16) of the resemblance matrix for extant abalone of Europe and West Africa, where shaded ellipses indicate the 95% confidence interval of group (species, subspecies, or population) centroids, and plot characters indicate data source. (**2–8**) Associations between ordination structure and morphometrics influencing this structure, where the thin black lines illustrate: (**2**) length; (**3**) height:length ratio; (**4**) width:length ratio; (**5**) height:width ratio; (**6**) relative spire position; (**7**) total tremata; (**8**) open tremata.

https://doi.org/10.1017/jpa.2024.50 Published online by Cambridge University Press

Table 1. Results of pairwise comparisons testing the hypotheses that there were no differences in central tendency (i.e., centroid) of shell form among the studied extant abalone groups (species, subspecies, or population of extant northeastern Atlantic and Mediterranean abalone). Statistic F is the ratio of the amount of variation between versus within groups, with the numerator and denominator each weighted by their degrees of freedom. It is 0 or positive, with larger values corresponding to larger proportional importance of the grouping factor. Holm-adjusted probability that the distance between centroids arose by random chance (p) is presented.

	H. tuberculata coccinea		*H. tuberculata fernandesi*		*H. tuberculata tuberculata*		*H. stomatiaeformis*	
Recent *Haliotis*	F	p	F	p	F	p	F	p
H. tuberculata fernandesi	4.82	0.0013	—	—	—	—	—	—
H. tuberculata tuberculata	16.21	0.0001	4.97	0.0007	—	—	—	—
H. stomatiaeformis	30.24	0.0001	7.02	0.0003	52.23	0.0001	—	—
H. tuberculata (Dakar)	7.37	0.0001	4.13	0.0035	2.71	0.0283	33.80	0.0001

Description. Small, ear-shaped shell (L_{max} = 25 mm) with rapidly increasing whorls. Spire not elevated, apex in subcentral position located 30–35% from the posterior margin. Dorsal surface ornamented with seven to eight well-defined spiral threads in early teleoconch, doubling in number in adult shell by the addition of secondary threads; spiral elements intersected by growth marks in early teleoconch, by closely spaced imbricate scales in late teleoconch. Elongated and slightly elevated tremata: five to six open, up to 19 total in larger shells. Thin, smooth spiral cord between the row of tremata and the peripheral carina. Flattened or slightly convex base with two to three fine parallel cords to columella. Columellar callus narrow, flattened.

Additional specimens. France, Miocene: ACC, three specimens, Landes, Meilhan carrière Vives (Burdigalian); ACC, two specimens, Landes, Campagne carrière Vives (Burdigalian); ACC, three specimens, Gironde, Pessac Lorient (Aquitanian); ACC, one specimen, Gironde, Martillac le Breyra (Burdigalian); MHNBx, one specimen, Gironde, Martillac (Burdigalian) (figured in Cossmann and Peyrot, 1917, pl. 10, fig. 3); NHMR, one

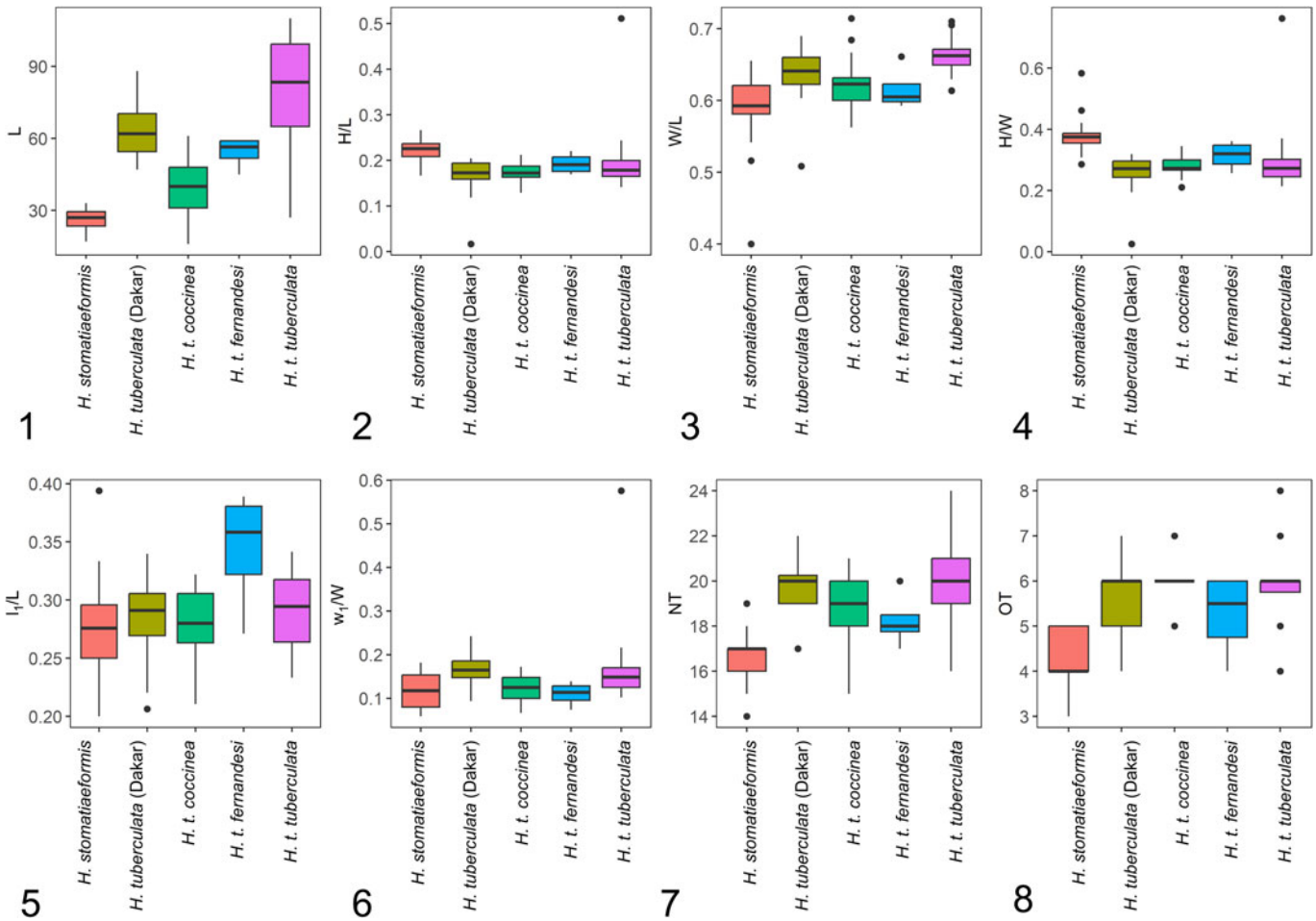

Figure 4. Box plots showing univariate comparisons among extant European and West African abalone species and subspecies. (**1**) Shell length. (**2**) Height:length ratio. (**3**) Width:length ratio. (**4**) Height:width ratio. (**5**) Relative spire position with respect to L. (**6**) Relative spire position with respect to W. (**7**) Total number of tremata. (**8**) Open tremata. Boxes illustrate first and third quartile as box edges and median as central line.

https://doi.org/10.1017/jpa.2024.50 Published online by Cambridge University Press

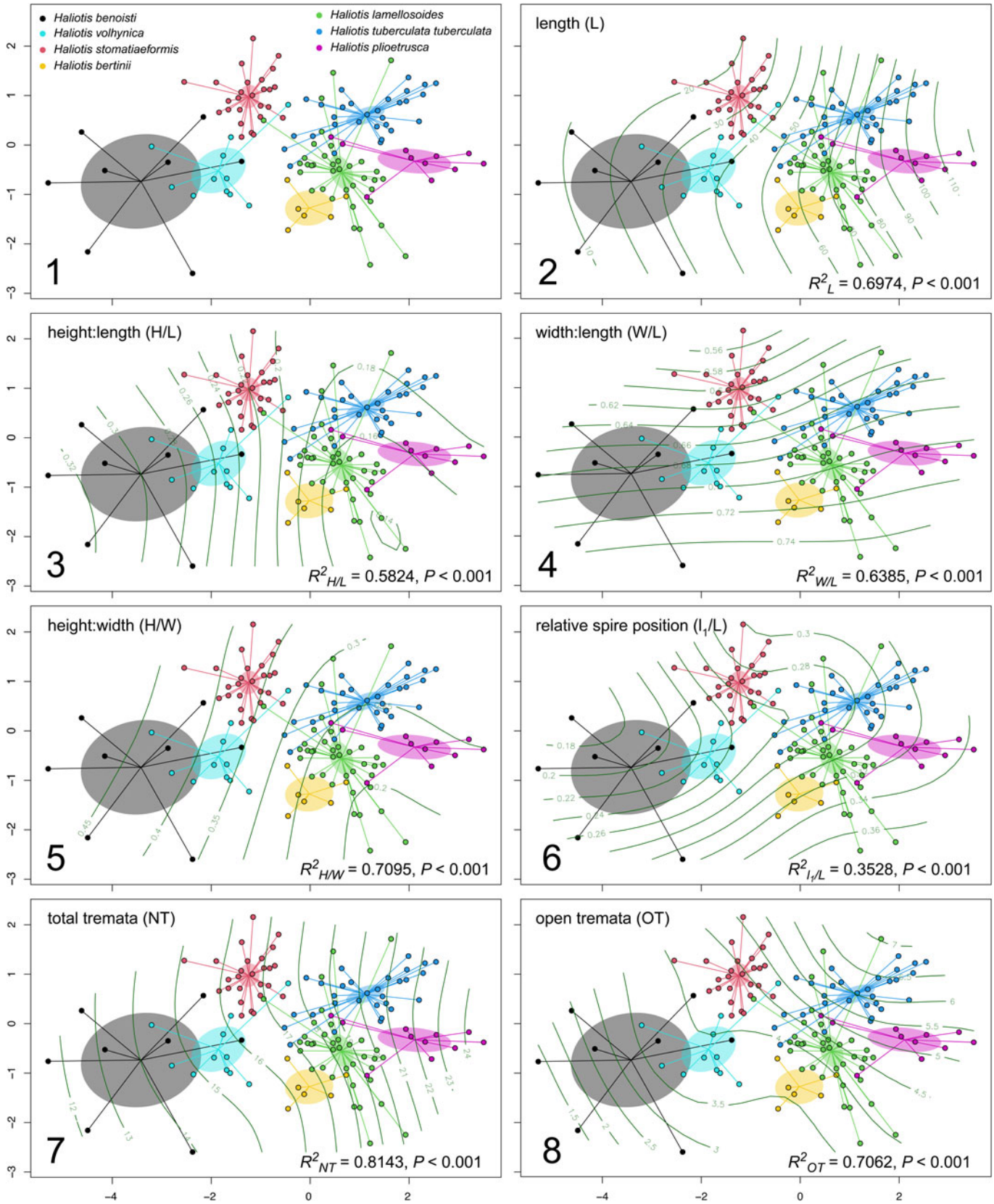

Figure 5. (**1**) nMDS ordination (stress = 0.16) of the resemblance matrix for fossil and extant abalone of Europe and West Africa, where shaded ellipses indicate the 95% confidence interval of group (species) centroids, and plot characters indicate data source. (**2–8**) Associations between ordination structure and morphometrics influencing this structure, where the thin black lines illustrate: (**2**) length; (**3**) height:length ratio; (**4**) width:length ratio; (**5**) height:width ratio; (**6**) relative spire position; (**7**) total tremata; (**8**) open tremata.

https://doi.org/10.1017/jpa.2024.50 Published online by Cambridge University Press

Table 2. Results of pairwise comparisons testing the hypotheses that there were no differences in central tendency (i.e., centroid) of shell form among the studied extant abalone groups (species or subspecies of fossil and extant European abalone). Statistic F is the ratio of the amount of variation between versus within groups, with the numerator and denominator each weighted by their degrees of freedom. It is 0 or positive, with larger values corresponding to larger proportional importance of the grouping factor. Holm-adjusted probability that the distance between centroids arose by random chance (p) is presented.

	H. volhynica		*H. benoisti*		*H. stomatiaeformis*		*H. bertinii*		*H. lamellosoides*		*H. plioetrusca*	
Fossil and Recent European *Haliotis*	F	p	F	p	F	p	F	p	F	p	F	p
H. benoisti	3.63	0.0023	—	—	—	—	—	—	—	—	—	—
H. stomatiaeformis	20.37	0.0001	18.56	0.0001	—	—	—	—	—	—	—	—
H. bertinii	8.91	0.0006	9.14	0.0004	21.58	0.0001	—	—	—	—	—	—
H. lamellosoides	27.09	0.0001	35.93	0.0001	51.68	0.0001	3.55	0.0066	—	—	—	—
H. plioetrusca	26.20	0.0001	27.42	0.0001	57.03	0.0001	8.48	0.0001	11.38	0.0001	—	—
H. tuberculata tuberculata	32.58	0.0001	42.49	0.0001	57.16	0.0001	12.88	0.0001	20.43	0.0001	7.92	0.0001

specimen, Nouvelle-Aquitaine, Vienne, Moulin Pochard (Langhian); JLC, one incomplete specimen, Gironde, Lariey (Aquitanian) (Lozouet et al., 2001b, p. 16, pl. 3, fig. 4).

Remarks. The species was introduced on the basis of five abraded specimens that are probably only fragments of a much larger original shell (see Cossmann, 1896). In a second paper, an adult specimen was figured (Cossmann and Peyrot, 1917). Geiger and Groves (1999) attributed Oligocene and early Miocene abalones of Aquitaine to *H. volhynica* Eichwald, 1853, in turn considered subspecies of *H. tuberculata* (Linnaeus, 1758). The multivariate analysis of shell forms based on type material and additional shells from several French localities confirms the separation from *H. volhynica*. Following Lozouet et al. (2001b), *Haliotis benoisti* is considered valid and applied to *Haliotis* from the late Oligocene and early Miocene of Aquitaine. The Oligocene record is from St.-Paul-Les-Dax, France (Geiger and Groves, 1999, and references therein).

Haliotis volhynica Eichwald, 1829
Figures 8.5–8.16, 9.1–9.5

1829 *Haliotis volhynica* Eichwald, p. 294, pl. 5, fig. 18.
1847 *Haliotis monilifera* Michelotti, p. 167, pl. 6, figs. 12, 12a.
1856 *Haliotis volhynica*; Hörnes, p. 510, pl. 46, fig. 26.
1897 *Haliotis tuberculata* var. *tauroparva* Sacco, p. 5, pl. 1, figs. 1–3.
1897 *Haliotis monilifera*; Sacco, p. 7, pl. 1, figs. 9–14.
1897 *Haliotis* ? *anomiaeformis* Sacco, p. 7, pl. 1, fig. 15 (nomen dubium).
1928 *Haliotis volhynica*; Friedberg, p. 530, pl. 34, figs. 8, 9.
1937 *Haliotis volhynica*; Davidaschvili, p. 540, pl. 1, fig. 5.
1949 *Haliotis* sp. Glibert, p. 12, pl. 1, fig. 1.
1954 *Haliotis tuberculata lamellosoides*; Csepreghy-Meznerics, p. 10, pl. 1, fig. 24.
1955 *Haliotis* (*Haliotis*) *volhynica*; Korobkov, pl. 2, fig. 3.
1960 *Haliotis* (*Haliotis*) *tuberculata* var. *lamellosoides*; Kojumdgieva and Strachimirov, p. 84, pl. 28, fig. 9.
1963 *Haliotis* sp. Steininger, p. 37, pl. 12, fig. 1.
1966 *Haliotis tuberculata volhynica*; Strausz, p. 26, fig. 16c.
1967 *Haliotis volhynica*; Bielecka, p. 132, pl. 8, figs. 3, 4 (fide Bałuk, 1975).
1968 *Haliotis volhynica*; Zelinskaya et al., p. 95, pl. 27, fig. 1.
1975 *Haliotis* (*Sulculus*) sp. Baluk, p. 22, pl. 1, figs. 4, 5.
1981 *Haliotis tuberculata*; Krach, p. 39, pl. 11, figs. 1–3.
1979 *Haliotis* (*Sulculus*) *volhynica*; Jakubowski and Musiał, p. 61, pl. 5, fig. 5.
2007 *Haliotis tuberculata*; Saint Martin et al., p. 43, fig. 5.
2012 *Haliotis tubercolata*; Górka et al., p. 163, figs. 7a, 15a, b.
2015 *Haliotis volhynica*; Forli et al., p. 89, figs. 2–14.
2017 *Haliotis volhynica*; Owen and Berschauer, p. 40, figs. 1–17; 1–15; 7; 10; 13; 16.

Type material. Holotype, NHMW A629. Type locality: Austria, north of Eggenburg, Gauderndorf, early Miocene (Mandic and Steininger, 2003) (Fig. 8.5–8.6).

Occurrence. Haliotis volhynica Eichwald, 1829 extends from the Western (Italy) to the Central and Eastern Paratethys (Austria, Romania, Bulgaria, Poland, Ukraine), ranging from the Burdigalian (Torino Hill, Italy) to the early Tortonian (Korytnica, Poland). It is

https://doi.org/10.1017/jpa.2024.50 Published online by Cambridge University Press

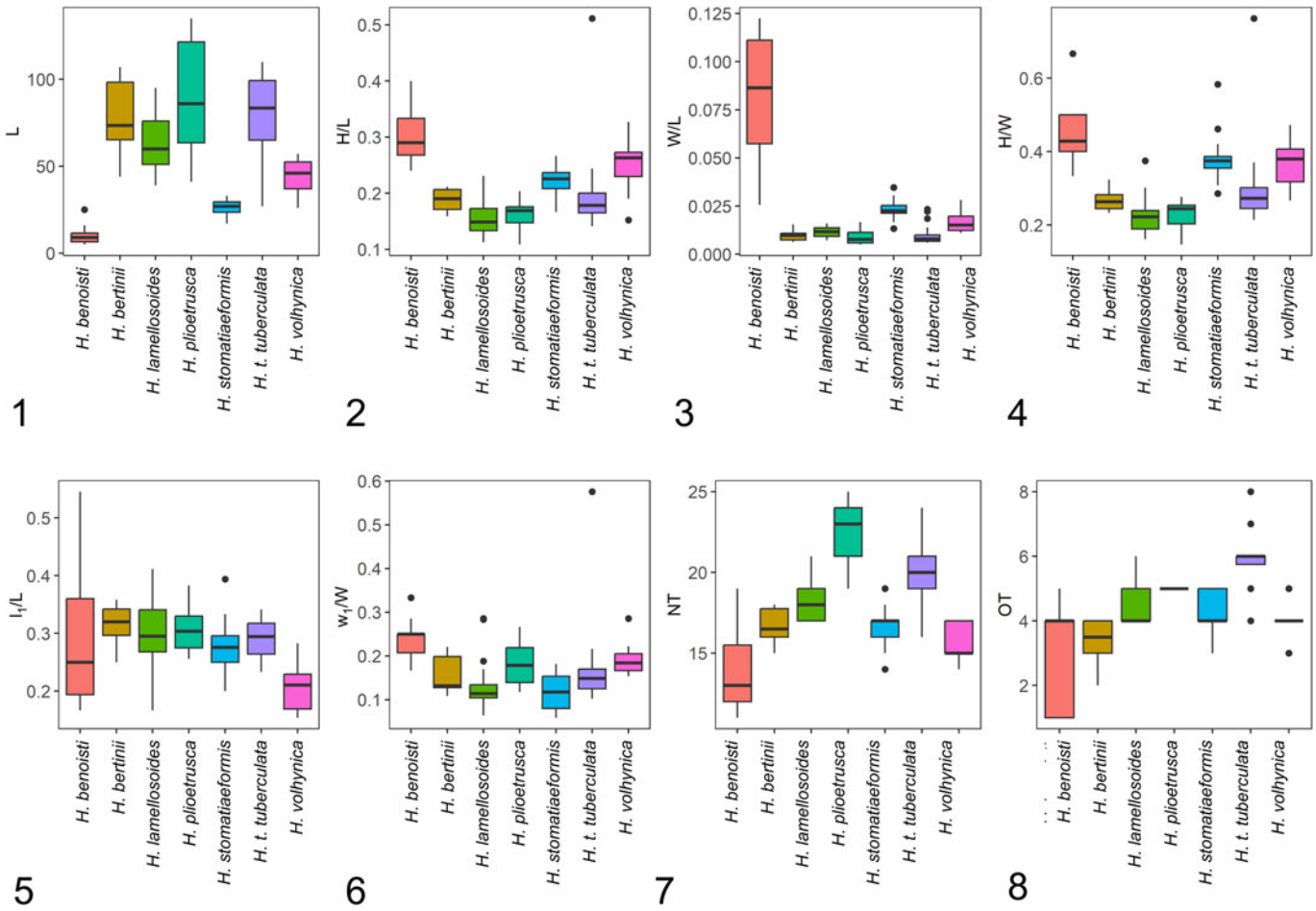

Figure 6. Box plots showing univariate comparisons among European known fossil and extant abalone species. (**1**) Shell length. (**2**) Height:length ratio. (**3**) Width:length ratio. (**4**) Height:width ratio. (**5**) Relative spire position with respect to L. (**6**) Relative spire position with respect to W. (**7**) Total number of tremata. (**8**) Open tremata. Boxes illustrate first and third quartile as box edges and median as central line.

particularly abundant in infralitoral organogenic limestones of Ukraine.

Description. Medium-sized, moderately convex oval shell (L_{max} = 70 mm). Spire moderately elevated, apex in subcentral position located 30–35% from the posterior margin. Grainy dorsal surface with spiral cords more or less broken up by radial folded ridges. Oval tremata: four to five open, up to 17 total in adult shell. Concave peripheral area between row of tremata and a prominent peripheral carina running parallel to columella. Columellar callus narrow, flattened.

Figure 7. (**1–5**) *Haliotis benoisti* Cossmann, 1896. (**1–3**) France, Gironde, Martillac, Miocene, Burdigalian. (**1–3**) MHNBx 2014.10.3910, L 25 mm, W 16 mm. (**4, 5**) Original labels. Scale bars = 5 mm (left) and 10 mm (right).

https://doi.org/10.1017/jpa.2024.50 Published online by Cambridge University Press

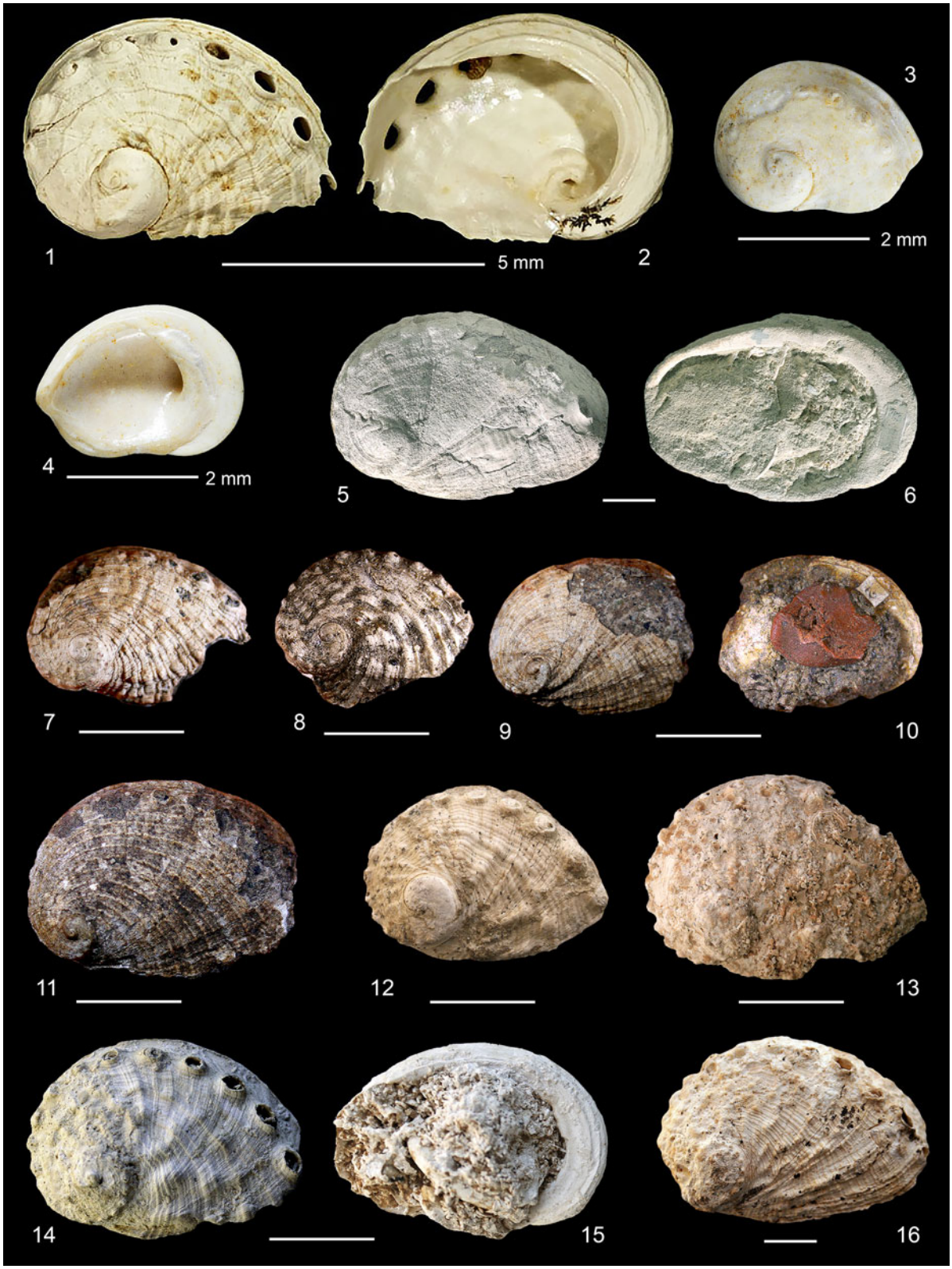

Figure 8. (**1–4**) *Haliotis benoisti* Cossmann, 1896. (**1, 2**) France, Vienne, southwest of Ambèrre, Moulin-Pochard, alongside D24, Miocene, Langhian, NHMR 6914, L 6 mm, W 4 mm. (**3, 4**) France, Gironde, Mérignac, Miocene, Aquitanian, holotype, MNHN.F.J04614, L 4 mm, W 2 mm. (**5–16**) *Haliotis volhynica* Eichwald, 1829. (**5, 6**) Austria, Horn District, Gauderndorf, Miocene, Badenian, NHMW A 629, L 5 mm, W 4 mm. (**7, 8**) Ex *Haliotis monilifera* Michelotti, 1847. Italy, Piedmont, Torino Hills, Miocene, Burdigalian. (**7**) MRSN BS.082.01.008, L 21 mm, W 15 mm. (**8**) MRSN BS.082.01.011, L 19 mm, W 15 mm. (**9–11**) Ex *Haliotis tuberculata* var. *tauroparva* Sacco, 1897. Torino Hills, Miocene, Burdigalian. (**9, 10**) MRSN BS.082.01.002, L 21 mm, W 14 mm. (**11**) MRSN BS.082.01.001, L 26 mm, W 20 mm. (**12**) Ukraine, Ternopil, Maksymivka, Miocene, Badenian, IGF 105317, L 23 mm, W 17 mm. (**13**) IGF 105318, L 27 mm, W 20 mm. (**14, 15**) IGF 105319, L 26 mm, W 19 mm, H 6 mm. (**16**) IGF 105320, L 52 mm, W 36 mm, H 17 mm. Unless otherwise indicated, scale bars = 10 mm.

https://doi.org/10.1017/jpa.2024.50 Published online by Cambridge University Press

Additional specimens. RMQ, one specimen, Poland, Korytnica, late Miocene, early Tortonian; 30 specimens, Ukraine, Ternopil, Maksymivka quarry, middle Miocene, Badenian.

Other fossil material. MRSN BS.082.01.001 (Fig. 8.11), 002 (Fig. 8.9, 8.10), Italy, Piedmont, Torino Hills, early Miocene, Burdigalian; MRSN BS.082.01.008 (Fig. 8.7), 009, 010, 011 (Fig. 8.8), Italy, Piedmont, Torino Hills, early Miocene, Burdigalian; MZB, one fragmentary specimen, Italy, Piedmont, Torino Hills, early Miocene, Burdigalian.

Remarks. Some authors considered *H. volhynica* Eichwald, 1829 a synonym of the widespread extant Mediterranean and Atlantic *H. tuberculata*, either as a distinct subspecies (*H. tuberculata volhynica*; Strausz, 1966; Geiger and Groves, 1999) or even as *H. tuberculata tuberculata* (Górka et al., 2012). General shell form allows us to clearly separate the two species (Figs. 5, 6). The morphological characteristics of *H. volhynica* are fairly constant and distinct: the apex moved toward the geometric center (Fig. 6.2; studied specimens allowed us to cover a wide range of sizes, enabling us to exclude the possibility that this difference is due to anisometric growth), the more rounded and tighter early teleoconch, and the ornamentation, consisting of marked tuberculate spiral cords (Csepreghy-Meznerics, 1954; Zelinskaya et al., 1968; Krach, 1981; Górka et al., 2012) differentiate it also from *H. lamellosoides*. The same diagnostic features are seen in molds (e.g., Friedberg, 1928; Strausz, 1966). *Haliotis tuberculata* var. *tauroplanata* Sacco, 1897 (Fig. 9.14–9.16) and *H. tuberculata* var. *lamellosoides* Sacco, 1897 (Fig. 10.1–10.3), from the Miocene and the Pliocene of northern Italy, respectively, possess slender and subequal spiral cords with small tubercles, whereas *H. volhynica* is more rounded and usually bears four to five open tremata, versus six to seven in *H. tuberculata*. *H. volhynica* found at Maksymivka (Ukraine) are well characterized and show a small degree of variability (Owen and Berschauer, 2017). *Haliotis monilifera* Michelotti, 1847, with more marked spiral ornaments and slightly larger tubercles that cross the growth lines (Fig. 8.7, 8.8), shares with *Haliotis volhynica* the general shape, the flattened columellar side, and the analogous number of respiratory holes. The same characters are seen in *Haliotis tuberculata* var. *tauroparva* Sacco, 1897 (Fig. 8.9–8.11) and the isolated specimen of *Haliotis anomiaeformis* Sacco, 1897 (p. 7, pl. 1, fig. 15; specimen now lost [D. Ormezzano, MRSN, personal communication, 2019]; the poor material upon which *H. anomiaeformis* was established does not help in establishing its validity, so it is here regarded as nomen dubium). The east African *Haliotis rugosa pustulata* Reeve, 1846 (Owen, 2013), recently introduced in the eastern Mediterranean via the Red Sea (Talmadge, 1971 Geiger, 1998, 2000; Zenetos et al., 2004), and the Indo-Pacific *Haliotis varia* Linnaeus, 1758, share with *H. volhynica* the general shell outline, the pattern of spiral growth, the ornamentation with pustules and elongated tubercles, and the shape of the columellar callus.

Haliotis stalennuyi Owen and Berschauer, 2017
Figure 9.6–9.8

1981 *Haliotis tuberculata tauroplanata*; Krach, p. 40, pl. 11, figs. 4–7.
2015 *Haliotis* sp.; Forli et al., p. 92, figs. 15–18.
2017 *Haliotis stalennuyi* Owen and Berschauer, p. 40, figs. 1–6; 8, 9; 11, 12; 14, 15.

Type material. Holotype: NMNZ, M.321138. Type locality: Ukraine, Ternopil, Maksymivka quarry.

Occurrence. Paratethys: middle Miocene, Badenian; Ukraine, Ternopil, Maksymivka (Forli et al., 2015; Owen and Berschauer, 2017); East Poland, Węglinek (Krach, 1981).

Description. Oblong shell of medium size (L_{max} = 60 mm), somewhat flattened and barely arched. Spire moderately flat to slightly elevated, apex in marginal position located 15–20% from the posterior margin. Smooth dorsal surface with spiral ribs almost entirely absent, with the exception of early teleoconch, where thin ribs and small tubercles are present. Shallow oval tremata, four to five open. Slightly rounded area, with three to four smooth cords, from the row of tremata and the peripheral carina.

Additional specimens. Type locality, middle Miocene, Badenian, one specimen, ASC, and one specimen, MSNF; middle Miocene, Badenian, one specimen, NHMW.

Remarks. *Haliotis stalennuy* is considered to differ from *H. vohlynica* by its different L/W ratio (1.79 and 1.46 respectively; Owen and Berschauer, 2017), giving rise to a wider early teleoconch, and by the different ornamentation, without radial folds and evident spirals cords. Differences in L/W ratio were not validated by the multivariate analysis due to lack of data (measures from only one specimen). In *H. stalennuyi*, the earliest teleoconch shows some slender spiral cords. Small tubercles are present in both species, but in *H. stalennuyi* they are present only in the first part of the teleoconch, whereas in *H. volhynica* they are present throughout life.

Haliotis ovata Michelotti, 1847
Figure 9.9–9.16

1847 *Haliotis ovata* Michelotti, p. 166.
1897 *Haliotis tuberculata*? var. *perspirata* Sacco, p. 5, pl. 1, fig. 4.
1897 *Haliotis tuberculata* var. *tauroplanata* Sacco, p. 6, pl. 1, fig. 5.
1897 *Haliotis ovata*; Sacco, p. 6, pl. 1, fig. 8.
1984 *Haliotis ovata*; Ferrero Mortara et al., p. 276, pl. 51, fig. 6a, b.

Type material. MRSN, BS.082.01.007. Type locality: Italy, Piedmont, Torino Hills, Miocene, Burdigalian.

Occurrence. Central Mediterranean, Italy, Piedmont, known only for the early Miocene (Burdigalian) of the Torinese Hills.

Description. Small shell (L_{max} = 40 mm), oval to oblong, moderately convex. Spire depressed, apex in peripheral position, located 10–15% from the posterior margin. Smooth dorsal surface with fine spiral striation. Tremata oval, not elevated, four open. Rounded peripheral area with four to five smooth cords, crossed by fine growth lines. Columellar callus large, flat.

Additional material. *Haliotis tuberculata*? var. *perspirata* Sacco, 1897, MRSN BS.082.01.003. Italy, Piedmont, Torino Hills, Miocene, Burdigalian. *Haliotis tuberculata var. tauroplanata* Sacco, 1897, MRSN BS.082.01.004. Italy, Piedmont, Torino Hills, Miocene, Burdigalian. NHMW, one specimen, Italy, Piedmont, Torino Hills, Miocene, Burdigalian.

Remarks. Michelotti (1847) wrongly figured a specimen of *H. monilifera*, not fitting with his description of *H. ovata*, which remains a valid species. The right type material was figured by

https://doi.org/10.1017/jpa.2024.50 Published online by Cambridge University Press

Figure 9. (**1–4**) *Haliotis volhynica* Eichwald, 1829. Ukraine, Ternopil, Maksymivka, Miocene, Badenian, IGF 105321, L 57 mm, W 38 mm, H 15 mm. (**5–8**) *Haliotis stalennuyi* Owen and Berschauer, 2017. Ukraine, Maksymivka, Miocene, Badenian. (**5**) IGF 105361, L. 60 mm, W 33 mm. (**6, 7**) IGF 105322, L 46 mm, W 27 mm. (**8**) Austria, NHMW, Miocene, Badenian, L 47 mm, W 34 mm. (**9–16**) *Haliotis ovata* Michelotti, 1847. Italy, Torino Hills, Miocene, Burdigalian. (**9–11**) MRSN BS.082.01.007, L 28 mm, W 20 mm, H 9 mm. (**12, 13**) Ex *Haliotis tuberculata* ? var. *perspirata* Sacco, 1897. Italy, Torino Hills, Miocene, Burdigalian. MRSN BS.082.01.003, L 14 mm, W 9 mm, H 4 mm. (**14–16**) Ex *Haliotis tuberculata* var. *tauroplanata* Sacco, 1897. Italy, Torino Hills, Miocene, Burdigalian. MRSN BS.082.01.004, L 41 mm, W 24 mm, H 7 mm. Scale bars = 10 mm.

https://doi.org/10.1017/jpa.2024.50 Published online by Cambridge University Press

Sacco (1897) (Fig. 9.9–9.11). *H. ovata* is distinguished from *H. tuberculata* by its flattened profile and the larger, flat columella.

Haliotis torrei Ruggieri, 1990

1990 *Haliotis* (*Sulculus*) *torrei* Ruggieri, p. 351, figs. 2, 3.

Type material. Holotype not found in the Ruggieri collection hosted at MGG in Palermo (C. D'Arpa, personal communication, 2024). Type locality: Italy, Sicily, Palermo, Petralia Sottana, late Miocene, Tortonian/Messinian.

Occurrence. The age determination is dubious. The sedimentary facies associated with the fossil is a calcareous marl with the colonial coral *Tarbellastrea* sp. The molluscan association suggests a late Tortonian age (Ruggieri, 1990, p. 351), but Petralia reefal carbonates of the Terravecchia Formation have also been attributed to the early Messinian (Grasso and Pedley, 1988; similarly to other analogous settings; Dominici et al., 2019).

Description. Small ear-shaped shell (L_{max} = 33 mm). Spire elevated, apex in peripheral position located about 20% from the posterior margin. Sloping dorsal surface, first a little convex after becoming flat near the carina, tessellated by nine large, flat, spiral cords crossed with deep growth lines. Oval tremata, elevated, four open. From the row of tremata and the peripheral carina, concave area with four to five small cords crossed by fine growth lines. Sinuous arched base with columellar callus narrow, rounded.

Remarks. The species is known only from the now lost holotype, and since its published image does not allow definitive taxonomic statements, the species should be considered a nomen inquirendum.

Haliotis lamellosoides Sacco, 1897
Figures 10–15

1897 *Haliotis tuberculata* var. *lamellosoides* Sacco, p. 6, pl. 1, figs. 6, 7.
1983 *Haliotis tuberculata lamellosoides*; Inzani, p. 12, figs. 1–8.
1992 *Haliotis tuberculata lamellosa*; Cavallo and Repetto, p. 36, fig. 17.
1998 *Haliotis tuberculata lamellosa*; Borghi and Vecchi, p. 83, pl. 1, figs. 1, 2.
2002 *Haliotis* (*Sulculus*) *quinquecentenaris* Lozano-Francisco and Vera-Peláez, p. 159, figs. A–D.
2003 *Haliotis iberica* Landau, Marquet, and Grigis, p. 11, pl. 2, figs. 3, 4.
2003 *Haliotis tuberculata*; Landau, Marquet, and Grigis, p. 12, pl. 2, figs. 1, 2.
2004 *Haliotis tuberculata lamellosa*; Chirli, p. 35, pl. 11, fig. 11.
2022 *Haliotis* (*Sulculus*) *quinquecentenaris* Vera-Peláez in Vera-Paláez and Lozano-Franisco, p. 26, pl. 3, figs. 10–12.
2022 *Haliotis tuberculata*; Vera-Peláez, p. 26, pl. 3, fig. 13.
2022 *Haliotis telescopica* Vera-Peláez, p. 27, figs. 14, 15.

Type material. MRSN BS.082.01.005, Italy, Piedmont, Asti, Colli Astesi, Pliocene, Piacenzian; BS.082.01.006, fragmentary, same data.

Emended diagnosis. Large *Haliotis* with a flat and large, slightly concave columellar callus and 17–19 total tremata, the last four to five of which are open.

Occurrence. West and Central Mediterranean. Pliocene, Zanclean: Italy, Siena, Montalcino, Quercecchio. Piacenzian: Italy, Piedmont, Asti, Colli Astesi; Emilia Romagna, Piacenza, Castell'Arquato; Tuscany, Pisa, Balconevisi; Siena, Bibbiano, Borgatello, Il Campino, Melograni, Pietrafitta, Podere Sant'Uliviere, Poggio alla Fame, Ponte a' Mattoni, Stroncoli. Spain: Malaga, Estepona.

Description. Ear-shaped to oval, large shell (L_{max} = 130 mm). Spire moderately flat to slightly elevated, apex in peripheral position located about 15–20% from the posterior margin. Moderately convex dorsal surface with highly variable ornamentation, from very fine spiral striation to 30–44 prominent and regularly spaced spiral cords, more or less broken up by radially folded ridges. Up to 21 oval tremata of medium size, round, somewhat elevated; last four to five tremata open. Sloping area from the row of tremata to the peripheral carina, with four to five cords crossed by growth lines. Base of whorl flat or gently arched, with large, flat, columellar callus.

Additional material. Italy, Tuscany: Siena, Montalcino, Quercecchio, Pliocene, Zanclean: two specimens. Siena, Castelnuovo Berardenga, Stroncoli, Pliocene, Piacenzian: 80 specimens. Siena, Castelnuovo Berardenga, Il Campino, Pliocene, Piacenzian: 15 specimens. Siena, San Gimignano, Podere Sant'Uliviere, Pliocene, Piacenzian: three specimens. Spain: Malaga, Estepona, Pliocene, Piacenzian: three specimens.

Remarks. Sacco (1897) proposed *Haliotis lamellosoides* as a variety of *H. tuberculata* and in connection with *H. lamellosa* Lamarck, 1822. Inzani (1983) separated the first two at the subspecies level. *H. lamellosoides* is here considered distinct from *H. tuberculata* Linnaeus, 1758 due to the flatter and larger, slightly concave columellar callus, the less-distinctly auriform outline, and the wider variety of ornaments. *H. lamellosoides* has a lower total number of tremata (17–19 versus 19–21 in *H. tuberculata*; Fig. 6.7) and lower number of open tremata (four on average versus six to seven in most *H. tuberculata*; Fig. 6.8). Specimens collected at Stroncoli show a wide range of variability (see juvenile, colored, and teratological specimens in Figs. 11.1–11.7, 15.16–15.19), with no solutions of continuity. This range includes forms described in the Piacenzian (Pliocene) of Estepona (Spain) and recently introduced as separated species. Larger and more rounded Terre Rosse specimens with wavy and interrupted spiral ornaments match *Haliotis iberica* Landau, Marquet, and Grigis, 2003 (specimens with prominent spiral cords widely spaced toward the periphery, interrupted at irregular intervals by radial fold, making them irregular and knobby; Figs. 12.11–12.13. 13.1–13.6. 14.1–14.5). Other specimens match with *Haliotis quinquecentenaris* Lozano-Francisco and Vera-Peláez, 2002 (specimens with very fine spiral cords, nearly smooth; Fig. 15.10–15.15) and others with *Haliotis telescopica* Vera-Peláez in Vera-Paláez and Lozano-Francisco, 2022, both also from Estepona. All the preceding reports from Estepona, southern Spain—here referred to *H. lamellosoides*—and its abundance in Tuscany, confirm that the species was widespread in the Mediterranean during the Piacenzian.

More convex, slightly smaller Terre Rosse specimens, bearing uniform spiral cords and lacking wavy plicae (Fig. 15.1–15.9), resemble *Haliotis tuberculata coccinea* Reeve, 1846, presently living in the Canary Islands and the Albora Sea. Molecular data indicate, however, that the latter diverged from a parental stock

https://doi.org/10.1017/jpa.2024.50 Published online by Cambridge University Press

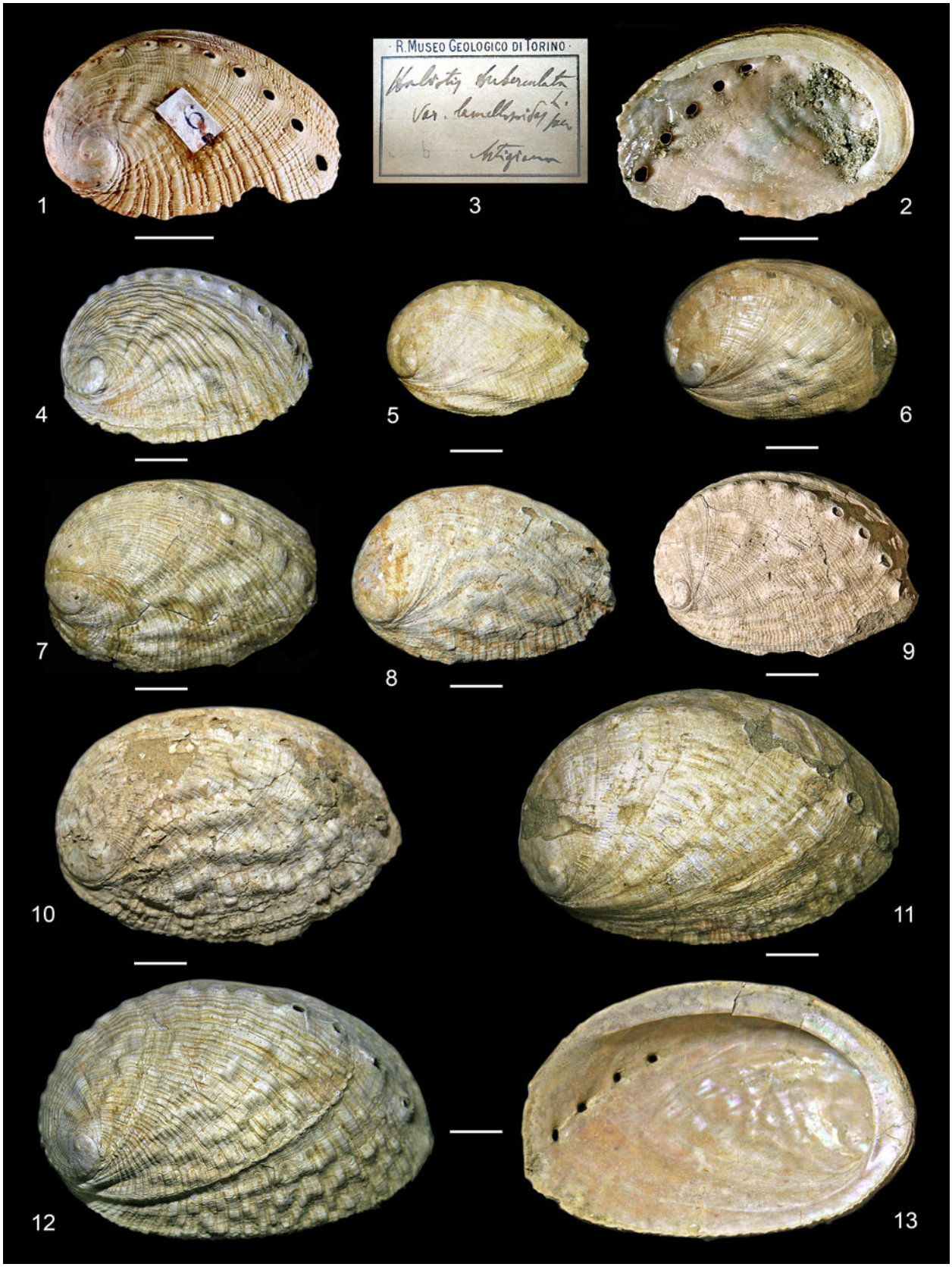

Figure 10. (**1–13**) *Haliotis lamellosoides* Sacco, 1897. (**1–3**) Italy, Piedmont, Asti, Colli Astesi, Pliocene, Piacenzian. (**1, 2**) Lectotype, MRSN BS.082.01.005, L 37.2 mm, W 25.3 mm. MRSN Original label. (**4, 6–8, 10–13**) Italy, Tuscany, Siena, Castelnuovo Berardenga, Stroncoli, Pliocene (Piacenzian). (**4**) IGF 105323, L 48 mm, W 34 mm. (**6**) IGF 105324, L 44 mm, W 31 mm. (**7**) IGF 105325, L 54 mm, W 36 mm. (**8**) IGF 105326, L 50 mm, W 35 mm. (**10**) IGF 105327, L 66 mm, W 46 mm. (**11**) IGF 105328, L 72 mm, W 49 mm. (**12, 13**) IGF 105329, L 72 mm, W 49 mm. (**5, 9**) Italy, Siena, Tuscany, Castelnuovo Berardenga, Il Campino, Pliocene (Piacenzian). (**5**) IGF 105330, L 39 mm, W 26 mm. (**9**) IGF 105331, L 50 mm, W 35 mm. Scale bars = 10 mm.

https://doi.org/10.1017/jpa.2024.50 Published online by Cambridge University Press

Figure 11. (**1–7**) *Haliotis lamellosoides* Sacco, 1897. Italy, Tuscany, Siena, Castelnuovo Berardenga, Il Campino, Pliocene (Piacenzian). (**1, 2**) *Pullus*, IGF 105356, L 2.5 mm, W 1.72 mm. (**3, 4**) Juvenile specimen, IGF 105357, L 7 mm, W 5.2 mm. (**5**) Juvenile specimen with little red flammae, IGF 105358, L 9.3 mm, W 5 mm. (**6**) Juvenile specimen, IGF 105359, L 10.8 mm, W 8.1 mm. (**7**) Juvenile specimen, IGF 105360, L 15 mm, W 10.5 mm. Unless specified, scale bars = 10 mm.

of *H. tuberculata* about 1.5 Ma (Van Wormhoudt et al., 2011), in the early Pleistocene. This datum is consistent with the Late Pleistocene report of *H. tuberculata coccinea* from Santa Maria Island, Azores (Avila et al., 2002), but not with the Tortonian, tentative identification of *Haliotis* from St-Clément-de-la-Place, Maine-et-Loire (northwestern France) (Landau et al., 2017, pl. 11, fig. 1).

Haliotis bertinii Forli, Dell'Angelo, Ciappelli, and Taviani, 2003
Figures 16.14, 16.15, 17.1–17.5

1952 *Haliotis tubercolata* var. *monilifera* Michelotti in Lecointre, p. 88, pl. 28, fig. 14.
2003 *Haliotis bertinii* Forli et al., p. 149, pl. 1, figs. 1–6, pl. 2, figs. 1–10.
2011 *Haliotis bertinii*; Chirli and Linse, p. 30, pl. 2, fig. 5a–c.
2022 *Haliotis bertinii*; Juárez-Ruiz and Mas, p. 243, fig. 10A,B.

Type material. Italy, Tuscany, Siena, Castelnuovo Berardenga, Stroncoli, Pliocene, Piacenzian. Holotype, MZB 25046, L 81.2 mm, W 59 mm, H 17 mm. Paratype 1, MZB 25041, L 65 mm, W 46 mm, H 12 mm. Paratype 2, MZB 25048, incomplete specimen. Paratype 3, FCC, L 111 mm, W 82 mm, H 18.4 mm. Paratype 4, FCC, L 107 mm, W 78.8 mm, H 21 mm. Paratype 5, FCC, L 66.2 mm, W 46.4 mm, H 10.5 mm. Paratype 6, MRC, L 105 mm, W 87 mm.

Occurrence. Atlanto-Mediterranean species reported at Morocco, Agadir, Pliocene (Lecointre, 1952); Spain, Baleares Islands, Pliocene, late Zanclean–Piacenzian, (Juárez-Ruiz and Mas, 2022); Italy, Siena, Stroncoli, Pliocene, Piacenzian (Forli et al., 2003); Greece, Rhodes Island, Pleistocene, Calabrian (Chirli and Linse, 2011).

Description. Ear-shaped, medium-large, and robust shell (L_{max} = 107 mm). Spire not much elevated, apex in peripheral position located about 20% from the posterior margin. Dorsal surface slightly convex at first, then gently sloping, nearly flat, crossed by small, regularly spaced and slightly tuberculated spiral cords. Last cord with oval holes, four open, form strong carina with protruding edge. The space between this last and the lower carina is slightly inclined, concave, and smooth, crossed only by growth lines. Flat and widened columellar edge fusing with the outer lip. The lip margin is narrow, arched, and convex.

Additional material. Five specimens, from type locality.

Remarks. The most distinctive character of this species is the presence of very strong, separated, and scaly spiral cords, with very little intraspecific variability across the geographic distribution (Rhodos Island, Balearic Islands, Morocco) and in time (Pliocene–Pleistocene; Chirli and Linse, 2011; Juárez-Ruiz and Mas, 2022; Lecointre, 1952) compared with that of *H. tuberculata*.

Haliotis plioetrusca new species
Figures 17.6, 17.7, 18, 19.1–19.4.

Type material and type locality. Holotype, MSNF IGF 105218, L 86 mm, W 57 mm. Paratype 1, MSNF IGF105219, L 115 mm, W 80 mm. Paratype 2, MSNF IGF 105220, L 130 mm, W 90 mm. Paratype 3, MSNF IGF 105231, L 70 mm, W 52 mm. Paratype 4, MSNF IGF 105232, L 41 mm, W 28 mm. Paratype 5, MSNF IGF 105233, L 46 mm, W 34 mm. Paratype 6, MSNF IGF 105234, L 57 mm, W 39 mm. Paratype 7, MSNF IGF 105235, L 128 mm, W 93 mm. Paratype 8, MSNF IGF 105236, L 79 mm, W 56 mm. Paratype 9, MSNF IGF 105237, L 135 mm, W 92 mm. Italy, Tuscany, Siena, Castelnuovo Berardenga, Stroncoli. Pliocene, Piacenzian.

Diagnosis. Large *Haliotis* with 20–25 tremata and fine, closely spaced spiral threads crossed by minute imbricate scales.

https://doi.org/10.1017/jpa.2024.50 Published online by Cambridge University Press

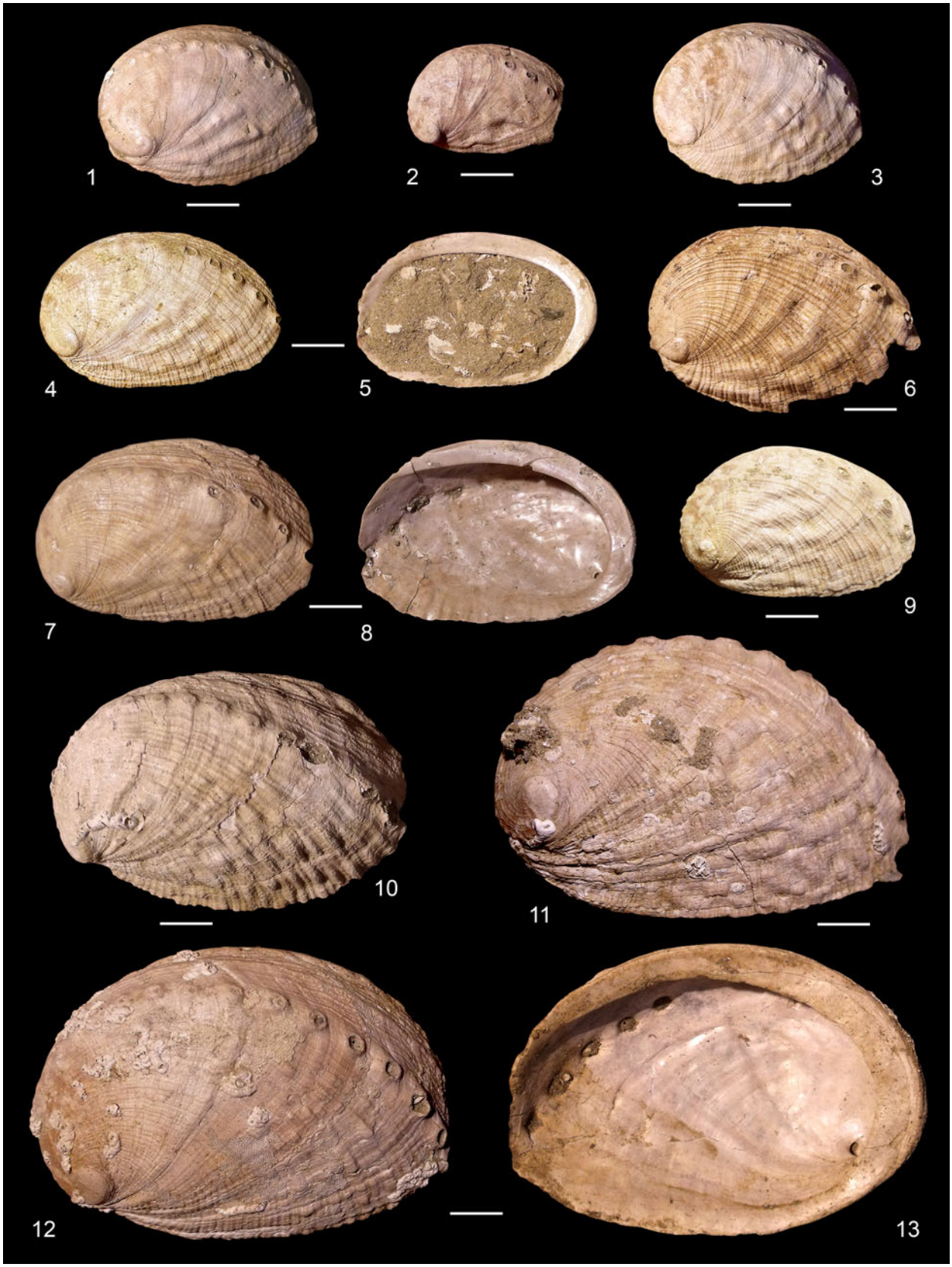

Figure 12. (**1–13**) *Haliotis lamellosoides* Sacco, 1897. Italy, Tuscany, Siena, Castelnuovo Berardenga, Stroncoli, Pliocene (Piacenzian). (**1**) IGF 105362, L 42 mm, W 31 mm. (**2**) IGF 105363, L 30 mm, W 21 mm. (**3**) IGF 105364, L 40 mm, W 31 mm. (**4, 5**) IGF 105365, L 46 mm, W 30 mm. (**6**) IGF 105366, L 52 mm, W 36 mm. (**7, 8**) GF 105367, L 53 mm, W 35 mm. (**9**) IGF 105368, L 44 mm, W 30 mm. (**10**) IGF 105369, L 68 mm, W 46 mm. (**11**) IGF 105370, L 79 mm, W 54 mm. (**12, 13**) IGF 105371, L 80 mm, W 56 mm. Scale bars = 10 mm.

https://doi.org/10.1017/jpa.2024.50 Published online by Cambridge University Press

Figure 13. (**1–7**) *Haliotis lamellosoides* Sacco, 1897. Italy, Tuscany, Siena, Castelnuovo Berardenga, Stroncoli, Pliocene (Piacenzian). (**1**) IGF 105372, L 95 mm, W 72 mm. (**2**) IGF 105373, L 67 mm, W 47 mm. (**3**) IGF 105332, L 73 mm, W 53 mm. (**4**) IGF 105374, L 97 mm, W 72 mm. (**5**) IGF 105333, L 77 mm, W 59 mm. (**6**) IGF 105375, L 102 mm, W 72 mm. (**7**) IGF 105334, L 54 mm, W 36 mm. Scale bars = 10 mm.

https://doi.org/10.1017/jpa.2024.50 Published online by Cambridge University Press

Figure 14. (**1–6**) *Haliotis lamellosoides* Sacco, 1897. (**1, 3–4, 6**) Italy, Tuscany, Siena, Castelnuovo Berardenga, Stroncoli, Pliocene (Piacenzian). (**1**) IGF 105335, L 94 mm, W 67 mm. (**3**) IGF 105336, L 111 mm, W 86 mm. (**4**) IGF 105376, L 52 mm, W 37 mm. (**6**) IGF 103388, L 88 mm, W 65 mm. (**2**) Italy, Tuscany, Siena, Castelnuovo Berardenga, Il Campino, Pliocene (Piacenzian), IGF 105337, L 58 mm, W 42 mm. Italy, Tuscany, Siena. Montalcino, Quercecchio, Pliocene (Zanclean). (**5**) IGF 105338, L 76 mm, W 59 mm. Scale bars = 10 mm.

https://doi.org/10.1017/jpa.2024.50 Published online by Cambridge University Press

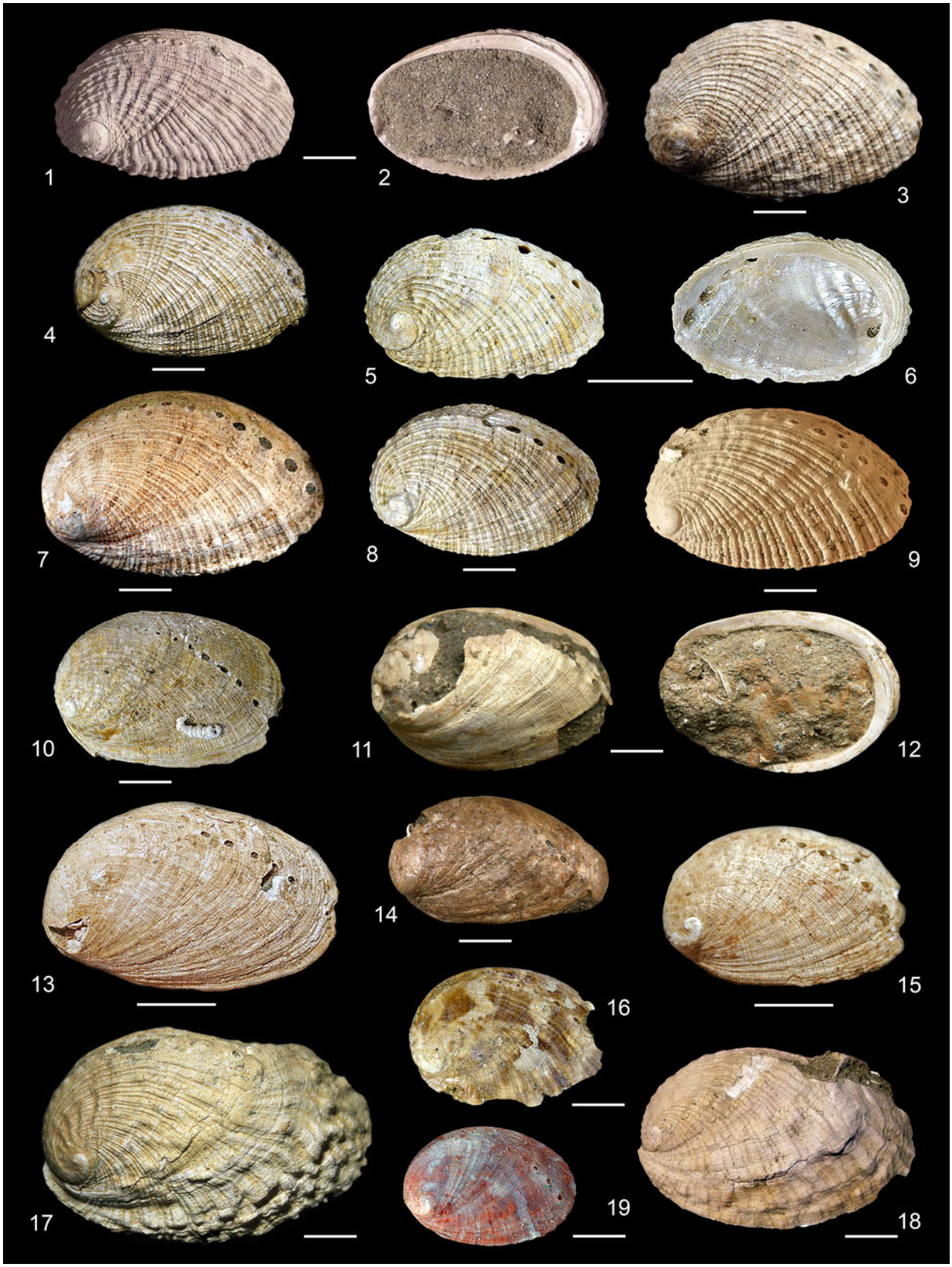

Figure 15. (**1–19**) *Haliotis lamellosoides* Sacco, 1897. Italy, Tuscany, Siena, Castelnuovo Berardenga, Stroncoli, Pliocene (Piacenzian). (**1, 2**) IGF 105377, L 44 mm, W 29 mm. (**3**) IGF 105339, L 53 mm, W 35 mm. (**4**) IGF 105340, L 45 mm, W 30 mm. (**5, 6**) IGF 105341, L 23 mm, W 16 mm. (**7**) MFC F036B 2901.53, L 54 mm, W 36 mm. (**8**) IGF 105378, L 44 mm, W 29 mm. (**10**) IGF 105379, L 44 mm, W 30 mm. (**11, 12**) IGF 105342, L 46 mm, W 31 mm. (**14**) IGF 105343, L 42 mm, W 24 mm. (**15**) IGF 105344, L 31 mm, W 21 mm. (**16**) Colored specimen, IGF 105380, L 37 mm, W 27 mm. (**17**) Teratological specimen, IGF 105345, L 63 mm, W 41 mm. (**18**) Teratological specimen, IGF 105381, L 53 mm, W 35 mm. (**19**) Colored specimen (highlighted color), IGF 105382, L 34 mm, W 23 mm. (**13**) Italy, Tuscany, Siena, Castelnuovo Berardenga, Il Campino, Pliocene (Piacenzian). IGF 105346, L 38 mm, W 24 mm. (**9**) Spain, Malaga, Estepona, Pliocene (Zanclean-Piacenzian), IGF 105387, L 51 mm, W 31 mm. Scale bars = 10 mm.

https://doi.org/10.1017/jpa.2024.50 Published online by Cambridge University Press

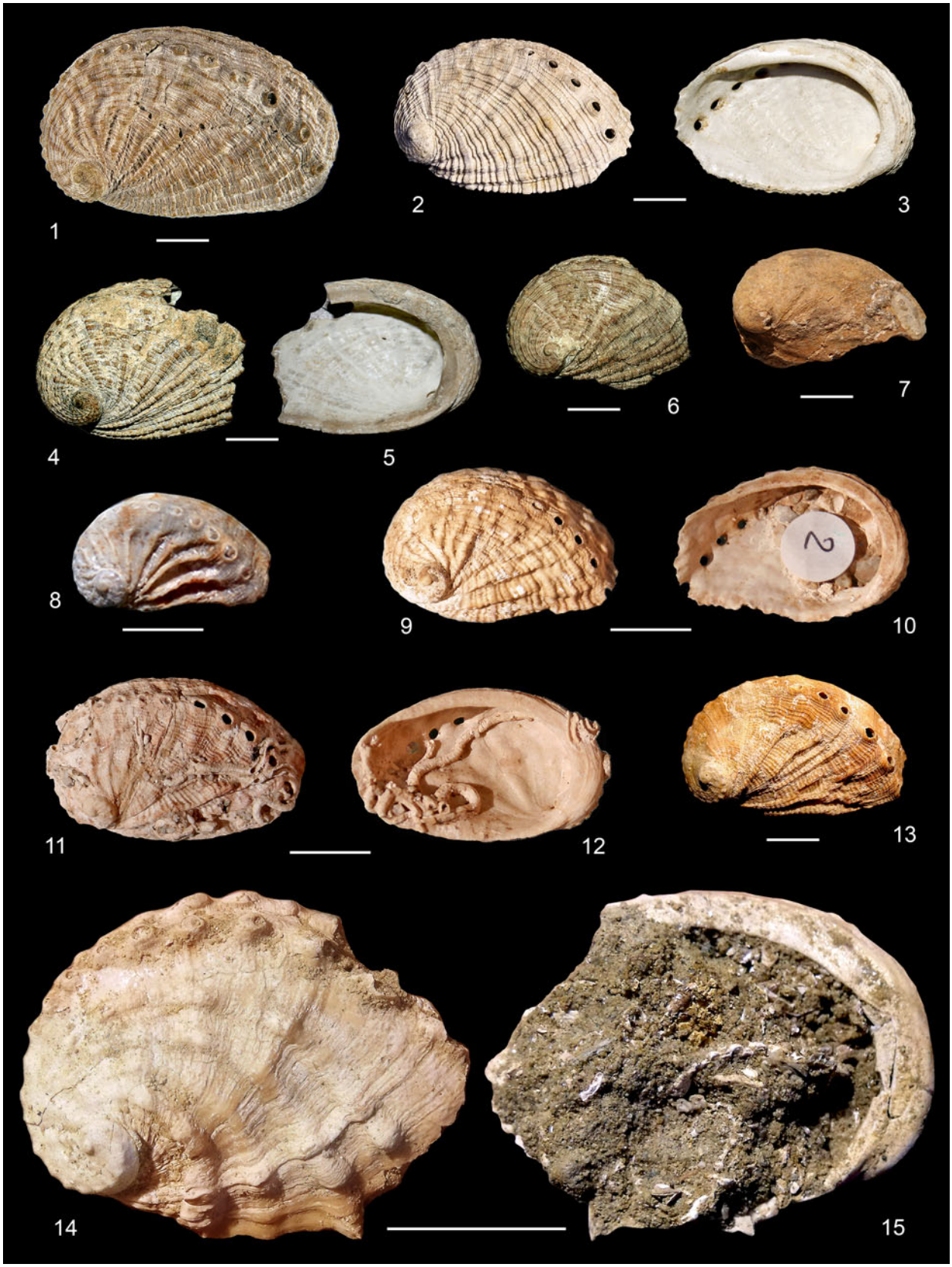

Figure 16. (**1–13**) *Haliotis tuberculata tuberculata* Linnaeus, 1758. (**1–6**) Italy, Lombardia, Milano, San Colombano, early Pleistocene (Gelasian). Ex *Haliotis prisca* De Cristofori and Jan, 1832. (**1**) Holotype, MSNM i 4288, L 57 mm, W 37 mm. (**2, 3**) MSNF IGF 105221, L 46 mm, W 30 mm. (**4, 5**) MSNF IGF 105222, L 40 mm, W 31 mm. (**6**) IGF 102117A, L 35 mm, W 26 mm. (**7**) Italy, Tuscany, Livorno, Rosignano Marittimo, Early Pleistocene (Calabrian), IGF 105348, internal cast, L 37 mm, W 23 mm. (**8**) Italy, Latina, Foce Verde, Late Pleistocene (Euthyrrenian). IGF 105347, L 19 mm, W 11 mm. (**9–12**) Italy, Calabria, Reggio Calabria, Bovetto, Late Pleistocene (Euthyrrenian). (**9, 10**) IGF 105349, L 30 mm, W 20 mm. (**11, 12**) IGF 105350, L 32 mm, W 20 mm. (**13**) Italy, Tuscany, Livorno, Lazzeretto, Middle Pleistocene. CBC, L 43 mm, W 27 mm. (**14, 15**) *Haliotis bertinii* Forli, Dell'Angelo, Ciappelli, and Taviani, 2003. Italy, Tuscany, Siena, Castelnuovo Berardenga, Stroncoli, Pliocene (Piacenzian). IGF 105383, incomplete specimen, L 34 mm, W 29 mm. Scale bars = 10 mm.

https://doi.org/10.1017/jpa.2024.50 Published online by Cambridge University Press

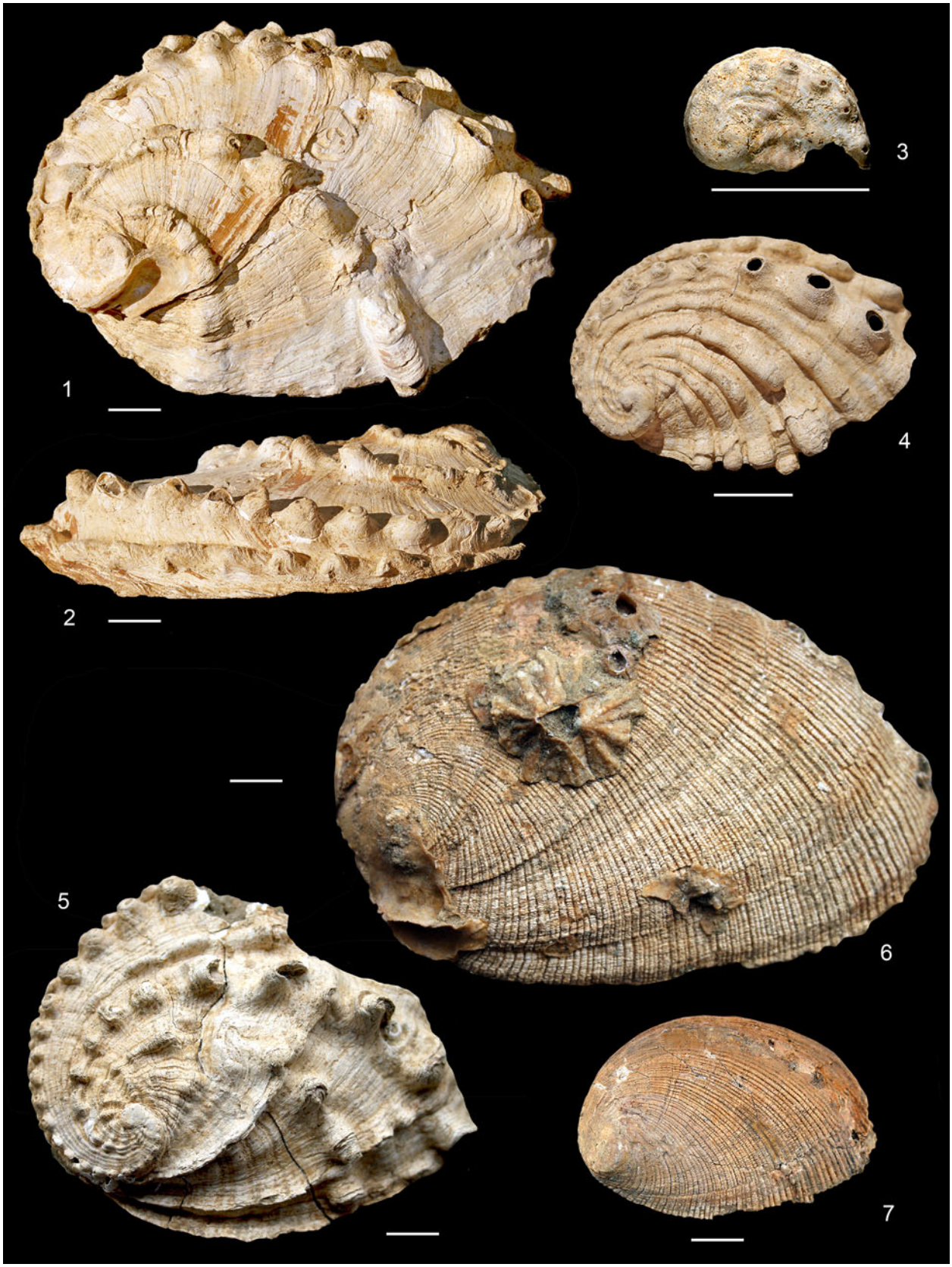

Figure 17. (**1–5**) *Haliotis bertinii* Forli, Dell'Angelo, Ciappelli, and Taviani, 2003. Italy, Tuscany, Siena, Castelnuovo Berardenga, Stroncoli, Pliocene (Piacenzian). (**1, 2**) IGF 105351, L 104 mm, W 68 mm. (**3**) Juvenile specimen, IGF 105384, L 12 mm, W 8 mm. (**4**) Juvenile specimen, IGF 105352, L 44 mm, W 30 mm. (**5**) IGF 105353, incomplete specimen, L 86 mm, W 67 mm. (**6, 7**) *Haliotis plioetrusca* n. sp. Italy, Tuscany, Siena, Castelnuovo Berardenga, Stroncoli, Pliocene (Piacenzian). (**6**) Paratype 1, IGF105219, L 115 mm, W 80 mm. (**7**) Paratype 6, IGF 105234, L 57 mm, W 39 mm. Scale bars = 10 mm.

https://doi.org/10.1017/jpa.2024.50 Published online by Cambridge University Press

Figure 18. (**1–8**) *Haliotis plioetrusc*a n. sp. Italy, Tuscany, Siena, Castelnuovo Berardenga, Stroncoli, Pliocene (Piacenzian). (**1, 2**) Paratype 2, MSNF IGF 105220, L 130 mm, W 90 mm. (**3**) Holotype, MSNF IGF 105218, L 86 mm, W 57 mm. (**4**) Paratype 3, MSNF IGF 105231, L 70 mm, W 52 mm. (**5**) Paratype 4, MSNF IGF 105232, L 41 mm, W 28 mm. (**6**) Paratype 5, MSNF IGF 105233, L 46 mm, W 34 mm. (**7–8**) *Haliotis marmorata* Linnaeus, 1758. Ghana, Terna, Recent. MMK 4586, L 37 mm, W 25 mm. Scale bars = 10 mm.

https://doi.org/10.1017/jpa.2024.50 Published online by Cambridge University Press

Figure 19. (**1–4**) *Haliotis plioetrusca* n. sp. (**1–3**) Italy, Siena, Castelnuovo Berardenga, Stroncoli, Pliocene (Piacenzian). (**1**) Paratype 7, MSNF IGF 105235, L 128 mm, W 93 mm. (**2**) Paratype 8, MSNF IGF 105236, L 79 mm, W 56 mm. (**3**) Paratype 9, MSNF IGF 105237, L 135 mm, W 92 mm. Italy, Tuscany, Siena, Montalcino, Quercecchio, Pliocene (Zanclean). (**4**) Incomplete specimen, IGF 105385, L 73 mm, W 64 mm. (**5–8**) *Haliotis marmorata* Linnaeus, 1758. Ghana, Busua Island, Recent. (**5, 6**) IGF 105354, L 40 mm, W 26 mm. (**7, 8**) IGF 105355, L 25 mm, W 17 mm. Scale bars = 10 mm.

https://doi.org/10.1017/jpa.2024.50 Published online by Cambridge University Press

Occurrence. Known only for the Tuscan Pliocene, at the type locality (Piacenzian), Siena, and near Montalcino, Siena, at Quercecchio (Zanclean).

Description. Large (up to 140 mm) auriform shell with a small, not elevated spire. Outer surface slightly convex, crossed by many spiral threads, subequal, equidistant. Tightly spaced growth increments cross spiral ornaments, forming minute, forward-leaning imbricate scales. Last five tremata open, with edge slightly elevated. Columellar callus wide, expanded, flat, connecting with convex, thin, crenulated outer lip. Internal surface smooth, without muscle scar.

Etymology. Named after the Pliocene Epoch and Latin adjective *etruscus*, derived from *Etruria*, an ancient Latin name for Tuscany.

Additional material. Three specimens, same locality as the holotype, including MZB, two incomplete specimens; BDA, one specimen. MCC, two incomplete specimens from Siena, Montalcino, Quercecchio, Pliocene, Zanclean.

Recent comparison material. H. marmorata Linnaeus, 1758: Ghana, Busua Island, MSNF IGF, two specimens. Ghana, Tema, MMK, two specimens. Gabon, Capo Esterias, MMK, two specimens (Fig. 1.5–1.8).

Remarks. H. plioetrusca n. sp. differs from all other Pliocene abalones by its larger size (Figs. 5.2, 6.1) and higher number of tremata (Figs. 5.7, 6.7). Superficially similar to *H. marmorata* from the tropical coasts of West Africa. The latter, however, is nearly half as large, with more spiral ornaments and a larger columellar callosity. Some incomplete specimens of *H. plioetrusca* have been found associated with *H. lamellosoides* also in a shoreface assemblage indicating a vegetated bottom (Quercecchio, Val d'Orcia basin, Zanclean, Pliocene; Dominici and Forli, 2021) (Fig. 19.4).

Haliotis stomatiaeformis Reeve, 1846

1846 *Haliotis stomatiaeformis*; Reeve, p. 73, fig. 74.
1848 *Haliotis neglecta* Philippi, p. 16.
2001 *Haliotis stomatiaeformis*; Geiger and Owen, p. 77, figs. 1–4.
2003 *Haliotis stomatiaeformis*; Owen, p. 287, pl. 1, 2.
2012 *Haliotis stomatiaeformis*; Geiger and Owen, p. 130, pl. 65, figs. 1–14.
2022 *Haliotis stomatiaeformis*; Chiappa et al., fig. 1E 2024 *Haliotis stomatiaeformis*; Reitano et al., figs 7–12.

Type material. Lectotype (BMNH 1950.3.16.22-24) and paralectotypes (BMNH: Geiger and Owen, 2001).

Occurrence. The species is rare in the Mediterranean; shells are found only along the rocky coasts of Sicily and Malta, and living specimens were collected under stones 2–3 m deep. Fossil near Grammichele, Catania, Italy, Late Pleistocene (Reitano et al., 2024).

Description. Small to medium, oblong to ovate shell (L_{max} = 45 mm), very convex. 20–37 smooth spiral cords between suture and row of tremata, stronger cords intercalated by one to three intermediary ones. Radially finely plicated, spire nearly terminal, elevated; three to five open tremata.

Remarks. One paratype is 45 mm long, but most specimens range 20–30 mm, with four open tremata on average (Geiger and Owen, 2001). Lives in sympatry with *H. tuberculata*, from which it can be distinguished: more elongated, more arched, strong spiral sculpture, no lamellae, smaller size (Geiger and Owen, 2012; Chiappa et al., 2022). Erroneously reported by Reeve (1846) from New Zealand, lives only in Malta and Sicily (rare).

Haliotis tuberculata Linnaeus, 1758
Figure 16.1–16.13

1758 *Haliotis tuberculata*; Linnaeus, p. 780.
1822 *Haliotis lamellosa* Lamarck, p. 217.
1829 *Haliotis tuberculata*; Eichwald, p. 294.
1832 *Haliotis prisca* De Cristofori and Jan, p. 3.
1846 *Haliotis lamellosa*; Reeve, pl. 14, figs. 14, 15.
1846 *Haliotis speciosa* Reeve, pl. 14, figs. 14, 15.
1846 *Haliotis tuberculata*; Reeve, pl. 39, fig. 34.
2001 *Haliotis mykonosensis* Owen et al., p. 301, figs. 1–4.

Type material. Six syntypes (LSL 576; Geiger and Owen, 20012).

Occurrence. H. tuberculata ranges the eastern Atlantic from the Channel, northwestern France, to Senegal, Gulf of Guinea, including Macaronesia, and the whole Mediterranean (Mgaya and Mercer, 1994; Chiappa et al., 2022). Fossil reports range from the early (Gelasian, San Colombano, northern Italy) to the Late Pleistocene (129–11.7 ka; Avila et al., 2002).

Description. Large shell (L_{max} = 123 mm; up to 102 mm in the Mediterranean; Geiger and Owen, 2012), from oval to ear-shaped, somewhat elongated, convexly depressed. Spire depressed to strongly elevated. Tremata medium sized, round, three to nine open, on average six. Deep spiral cords crossed by radial tubercles or lamellae, but highly variable from smooth with faint radial folds to sharp radial lamellae. Columella narrower than medium width.

Remarks. Haliotis tuberculata differs from *H. lamellosoides* by its narrower and somehow convex columella and by a higher number of tremata. Three subspecies are recognized on morphological grounds (Owen et al., 2015): *H. tuberculata tuberculata* (much larger than the other subspecies but also larger than *H. lamellosoides*; Fig. 4.1), *H. tuberculata coccinea* (Reeve, 1846), and *H. tuberculata fernandesi* Owen and Afonso, 2012. A separation of the first two is confirmed on molecular grounds (Chiappa et al., 2022). The status of *H. tuberculata fernandesi*, however—largely overlapping in shell form with *H. t. coccinea* (Fig. 3), the two differing only in ornamentation (Owen et al., 2015)—needs a molecular validation. *H. speciosa* Reeve, 1846 from Senegal has been placed in synonymy with *H. tuberculata* (Owen, 2006), an interpretation confirmed by the multivariate approach to shell form (Fig. 3).

https://doi.org/10.1017/jpa.2024.50 Published online by Cambridge University Press

Discussion

Adaptations in Mediterranean Haliotis. The site of Stroncoli provided the largest abundance of abalones among all known European fossil localities and the evidence of the coexistence of three species at one time and space, evidenced by pristine shells sampled in a laterally limited outcrop of an individual event bed. The co-occurrence here of well-preserved representatives in the families Patellidae and Haliotidae testifies to the proximity of the shoreline and the presence of a rocky substrate (Forli et al., 2003, 2004). Three species of *Haliotis* co-occurring in just one single shell bed is an exceptional feature even with respect to syntopic abalones in the Recent. Modern occurrences of *Haliotis* in the Mediterranean and eastern Atlantic indicate that, although two species may occur sympatrically in Sicily, Lampedusa and Malta, where the distribution of *H. tuberculata* overlaps with that of *H. stomatiaeformis* (Chiappa et al., 2022), only one species is reported at any one site. The morphotype "*H. mykonosensis*," with its thin, oblong to ovate, from flat to slightly convex shell, generally with five to six open tremata and an average adult size of about 40–48 mm (Crocetta and Rismondo, 2009; Geiger and Owen, 2012), does not correspond to any of the Terre Rosse morphologies herein described, neither is its validity corroborated by molecular data (Chiappa et al., 2022). More than one species may coexist at many other places, for example, in West Africa, where the area inhabited by *H. tuberculata* overlaps that of *H. marmorata* (Fig. 20), and at Rottnest Island, off northwestern Australia, Indian Ocean. where temperate seagrass and reef-building corals co-occur, contributing to a variety of microhabitats and where at least three species of abalones are reported (Geiger, 2000; Invert E Base, 2023; Wells et al., 2023). At Port Alfred, along the coast of South Africa, up to five species of abalones can coexist in sympatry (Bester-van der Merwe et al., 2012). Other discrete regions with endemic species, in the North Pacific (seven species) and New Zealand (three species), are similarly associated with temperate climates (Geiger, 2000; Estes et al., 2005). Camouflage and cryptic behavior typical of abalones (Searcy-Bernal and Gorrostieta-Hurtado, 2007; Cenni et al., 2010; Kim et al., 2020) in closely coexisting microhabitats of the indented and rugged late Pliocene coastline of Tuscany (Nalin et al., 2016) may thus explain the exceptionally high diversity encountered at Stroncoli. This is not unexpected, for high species richness of Mediterranean herbivore gastropods is associated with the mid-Piacenzian Warm Period (Dominici and Danise, 2023).

Relationships between Mediterranean and East Atlantic Haliotis.—The multivariate analysis of shell form and the systematic and stratigraphic review highlight the presence of two main groups of European fossil and Recent *Haliotis*. These data, based on a large number of specimens from many localities, coupled with known genetic relationships between extant forms, allow hypotheses on species-level evolutionary relationships. One group comprises specimens distributed in the Oligocene and Miocene of western and central Europe (*H. benoisti* and *H. volhynica*). The other connects Pliocene, Pleistocene, and Recent Mediterranean and West African species (*H. lamellosoides*, *H. bertinii*, *H. plioetrusca* and *H. tuberculata*; Fig. 5). The multivariate statistical comparison of shell form confirms that *H. volhynica* and *H. lamellosoides* represent two distinct species and that both can be clearly separated also from *H. tuberculata tuberculata* on the basis of the number of tremata and general size, larger in the second (Fig. 6). Both *H. volhynica* and *H. lamellosoides* average four open tremata (Fig. 6.8), but *H. lamellosoides* can be distinguished on a higher total number of tremata (Fig. 6.7).

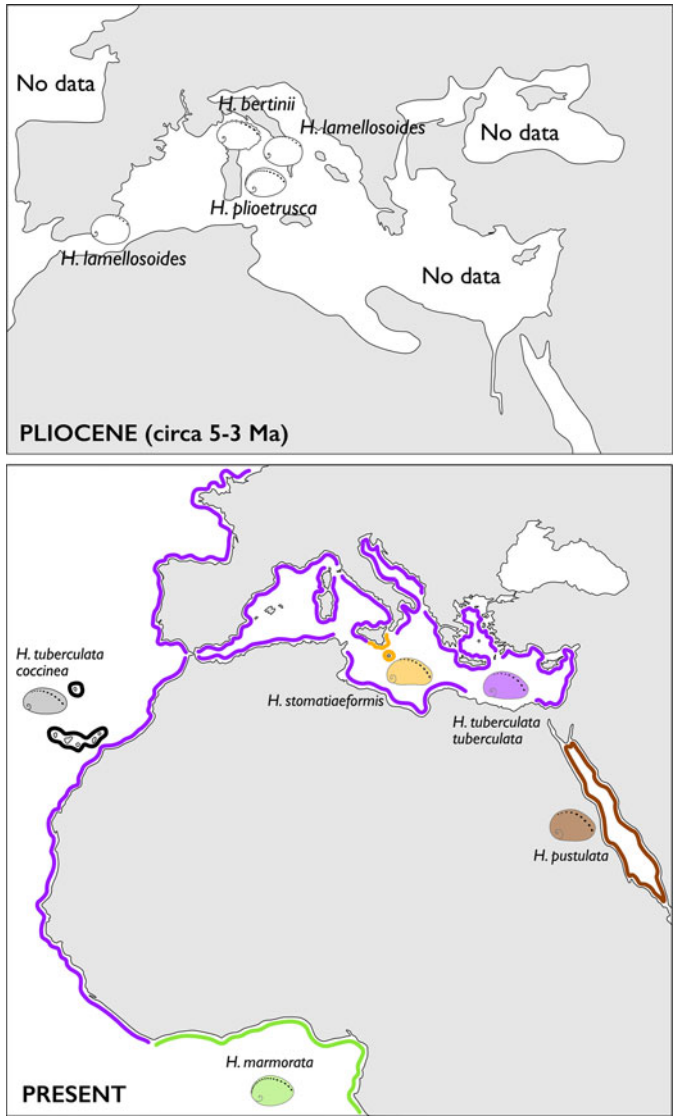

Figure 20. Distribution of species of *Haliotis* in the Mediterranean Pliocene and on the modern coasts of southern Europe, the Middle East, the Red Sea, and West Africa. *H. tuberculata coccinea* is very common also in the Azores, not included in the map. *H. tuberculata fernandesi* is restricted to Cape Verde, also not included.

The Miocene group includes (1) the possible ancestral form *H. benoisti* Cossmann, 1896 from the Oligocene–early Miocene of the northeastern Atlantic coast, (2) the younger *H. volhynica* from the early Miocene of western Paratethys, expanding its range eastward in the middle Miocene, joined by (3) *H. stalennuyi* Owen and Berschauer, 2017 (Figs. 21, 22). The multivariate analysis of shell form indicates that extant Mediterranean *H. stomatiaeformis* is more similar to Miocene *H. benoisti* and *H. volhynica* than to the sympatric *H. tuberculata tuberculata* (Fig. 5; Table 2; the latter with a record not older than the early Pleistocene). This could mean that the direct ancestor of *H. stomatiaeformis* is not *H. tuberculata* but an older form closer to the *H. benoisti–H. volhynica* lineage. The fact that in molecular phylogenies *H. stomatiaeformis* clusters with *H. tuberculata* and the Senegalese *H. marmorata* Linnaeus, 1758 (Van Wormhoudt et al., 2009; Chiappa et al., 2022) reveals only that the latter

https://doi.org/10.1017/jpa.2024.50 Published online by Cambridge University Press

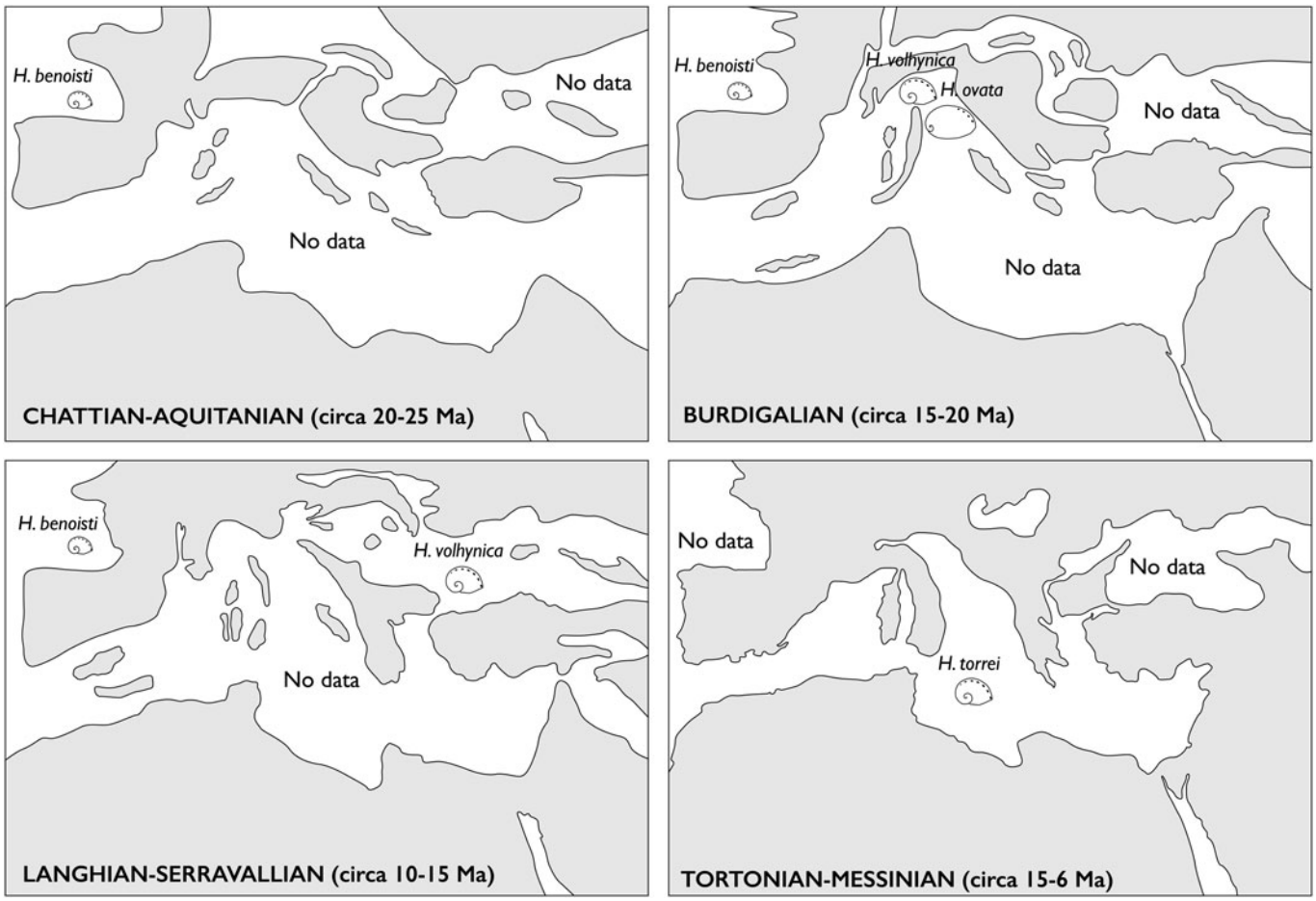

Figure 21. Oligocene–Miocene distribution of species of *Haliotis* in the Atlantic, Mediterranean, and Paratethys.

three extant species are ultimately rooted in the *H. benoisti–H. volhynica* lineage. The proximity in shell form of *H. lamellosoides* and *H. tuberculata* (Fig. 5) suggests that the first could be the direct ancestor of the second. A candidate ancestral form of all the three species found at Terre Rosse is *H. ovata* Michelotti, 1847, found in the early Miocene of western Paratethys (Fig. 22). The high morphological disparity recorded in *H. lamellosoides* and its association with *H. bertinii* and *H. plioetrusca* roughly coincide with an interval of high overall Mediterranean species richness recorded around the Zanclean–Piacenzian passage and in the first part of the Piacenzian (Aguirre et al., 2005; Dominici and Danise, 2023). *H. bertinii* and *H. plioetrusca* are now extinct. Tropical *H. marmorata* living in West Africa at subtropical and tropical latitudes (Fig. 20), limited southward by the Angola–Benguela Front, a major biogeographic boundary since the Miocene (Sessa et al., 2013, shows superficial similarities with *H. plioetrusca* (Fig. 19), pointing to possible phylogenetic relationships. The smaller size of the extant species would confirm the tendency for ectotherms to be smaller in warmer habitats (Dominici et al., 2020).

The contiguous, non-overlapping record of *H. lamellosoides* and *H. tuberculata* suggests that the second originated by anagenesis (Fig. 21), when Mediterranean climate shifted from tropical to temperate at the onset of the Northern Hemisphere Glaciation. *H. tuberculata* expanded its range from temperate regions southward along the Atlantic coast to its modern distribution. The present-day occurrence of endemic forms at Atlantic and Mediterranean islands (Fig. 20) indicates that species of *Haliotis*—like all stenotopic species confined to the shallow zone (Holland and Christie, 2013; Dominici and Danise, 2023)—are sensitive to successive eustatic cycles.

Morphological data retrieved from fossil shells thus show that a possible order of divergence of Mediterranean and eastern Atlantic abalones, from a longstanding, original stock of *H. lamellosoides*, is *lamellosoides–plioetrusca* by splitting, *lamellosoides–tuberculata tuberculata*– by anagenesis, and *tuberculata tuberculata–tuberculata coccinea* by splitting, a hypothesis corroborated by molecular data collected in living abalones (Van Wormhoudt et al., 2009, 2011; Chiappa et al., 2022). The fossil record indicates that Pleistocene climate change, as it did with other benthic mollusks (Mondanaro et al., 2024), played a major role in the geographic distribution of European abalones (Roussel and Van Wormhoudt, 2017).

The eastern connection. Molecular phylogenetic analyses and chromosome evidence suggest that the modern biodiversity abalone hotspot, centered in the tropical Indo-Pacific (Geiger, 2000), originated from Tethyan ancestors (Geiger and Groves, 1999; Estes et al., 2005; Bester-van der Merwe et al., 2012). The oldest group of European fossils herein discussed hints at an established eastern connection between the Mediterranean and the Indo-Pacific province through *H. volhynica*. The youngest report of *H. volhynica* is from the early Tortonian of the

https://doi.org/10.1017/jpa.2024.50 Published online by Cambridge University Press

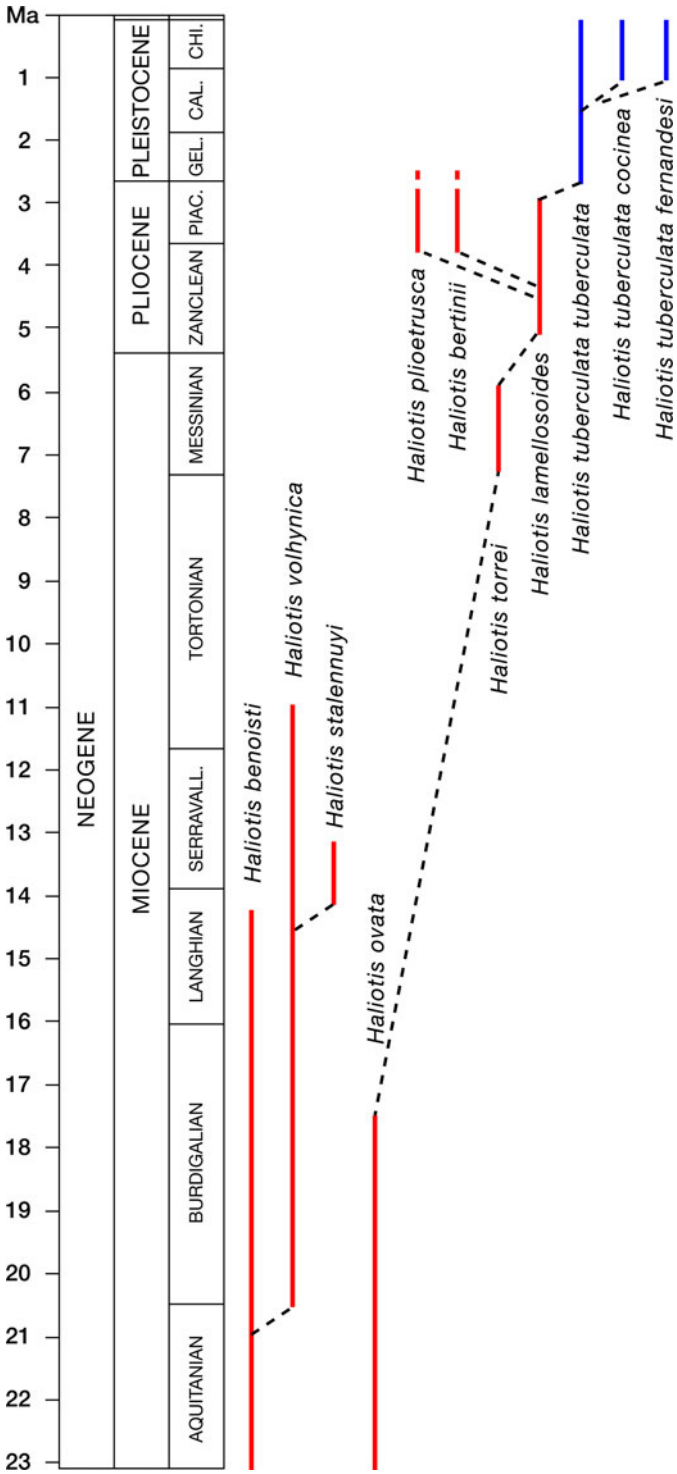

Figure 22. Species- and subspecies-level range of *Haliotis* in Europe during the Neogene. Tropical and subtropical species in red; temperate species in blue. Dashed lines indicate possible evolutionary relationships.

Paratethys, well after the closure of the Tethyan seaway during the early Miocene, at around 19 Ma (Yasuhara et al., 2022), and no evidence exists of extant Mediterranean descendants. Morphological affinities with recent immigrants from the Red Sea (small size, tight spiral growth originating shells with an oval outline, spiral ornaments with pustules or tubercles) are encountered with the East African and Indo-Pacific *H. rugosa pustulata* Reeve, 1846 and *H. varia* Linnaeus, 1758, presently ranging from Israel to East Africa, Persian Gulf, Red Sea, Madagascar, and Sri Lanka to Tonga, southern Japan, Philippines, and northwestern and western Australia (Geiger and Owen, 2012). Their fossil record is relatively young (Pleistocene of Egypt, Sudan, Zanzibar, and Tanzania for *H. rugosa pustulata*; Pliocene of Sri Lanka for *H. varia*; Geiger and Owen, 2012), and a phylogenetic relationship with *H. volhynica* can be hypothesized.

The middle Miocene (c. 16 Ma) *Haliotis amabilis* (Itoigawa and Tomida, 1982) from Japan instead shares morphological characters, including general form, dimensions, ornaments, and the presence of a flat columellar callous, with *H. ovata* and *H. lamellosoides* (compare with Tomida et al., 2006, fig. 2.1–2.3), hinting at an older Miocene center of diffusion. The fossil record of other large herbivore gastropods (Dominici et al., 2020) and large benthic species in general (Yasuhara et al., 2022) corroborates the hypothesis of a Miocene Tethyan center of origin of the modern diversity hotspot. The oldest fossil record of the family (two Late Cretaceous species from California) points to an even older, north-eastern Pacific origin of the clade (Groves and Alderson, 2008). Expansion possibly took place during the Paleogene in a greenhouse world, via the Atlantic at the time connected to the Pacific (Barnet et al., 2020).

Conclusions

New fossil finds of abalones in Tuscany add to the known Pliocene richness of *Haliotis* in the Mediterranean, peaking at a single site to the three species *Haliotis lamellosoides*, *H. bertinii*, and *H. plioetrusca*. A multivariate analysis of shell form of the European fossil and modern record of abalones, including morphometrics of 379 specimens from 17 countries in Europe and Africa, allows us to reassess the species- and subspecies-level taxonomy of *Haliotis* during the Neogene and the Quaternary. Merging new data with the known chronostratigraphic and paleogeographic distribution of fossil and extant species, two lines of descent are proposed. The first connects *H. benoisti* (Oligocene–early Miocene, northwestern Atlantic), *H. volhynica* (early–middle Miocene, Paratethys), *H. stalennuyi* (middle Miocene, Paratethys), *H. torrei* (late Miocene, Sicily), and *H. stomatiaeformis* (Recent, Sicily, Lampedusa, and Malta). The second possibly connects *H. ovata* (early Miocene, Paratethys), *H. torrei* (late Miocene), *H. lamellosoides* (Pliocene, Mediterranean), *H. bertinii* (late Pliocene, Mediterranean), *H. plioetrusca* (late Pliocene), *H. marmorata* (Recent, western Atlantic), *H. tuberculata tuberculata* (Gelasian–Recent, Mediterranean and western Atlantic), and *H. tuberculata coccinea* (late Pleistocene–Recent, western Atlantic). The available record justifies a hypothesis of diversification in the Mediterranean during a late Pliocene warmer interval, leading from *H. lamellosoides* to *H. bertinii* and *H. plioetrusca*, then from *H. lamellosoides* to *H. tuberculata* at the onset of climatic cooling, at the Pliocene–Pleistocene boundary.

Acknowledgments. Special thanks to A. Cluzaud (Pessac, Gironde, France), the personnel of the Muséum d'Histoire Naturelles de Bordeaux (France), J.-F. Lesport (Sainte-Hélène, Gironde, France), J.-M.l Pacaud (Muséum National d'Histoire Naturelle Paris, France), M. Harzhauser (Natural History Museum of Wien, Austria), A. Bonfitto, B. Sabelli (Museo dell'Evoluzione di Bologna, Italy), D. Ormezzano (Museo Regionale di Scienze Naturali di Torino, Italy), C. D'Arpa (Museo G.G. Gemmellaro, Palermo, Italy), G. Bini, and B. Santucci (Associazione Malakos, Città di Castello, Perugia, Italy) for their

https://doi.org/10.1017/jpa.2024.50 Published online by Cambridge University Press

assistance with collections hosted in their facilities. We are indebted to D. Bertini (Firenze), C. Bogi (Livorno), C. Chirli (Tavarnelle, Firenze), F. Ciappelli (Calenzano, Firenze), M. Cresti (San Casciano, Firenze), B. Dell'Angelo (Genova), S. Gori (Livorno), M. Rocca (Torino), C. Sbrana (Livorno), and A. Ventura (Colle val d'Elsa, Firenze) for sharing the results of their fieldwork on Neogene outcrops in Italy, and M. McCulloch (Sidney), J. Trotter (Sidney), and B. Gualandi (Bologna) for the trip at Rottnest Island, Australia. A. Mondanaro (Florence) and A. Tomašových (Bratislava) helped with statistical analyses. Finally, our sincere thanks to an anonymous reviewer and D. Geiger, whose detailed reviews helped to improve the quality of the article. This is Ismar-CNR, Bologna, scientific contribution n. 2094.

Competing interests. The authors declare none.

Data Availability Statement. Data available from the Dryad Digital Repository: https://doi.org/10.5061/dryad.4b8gthtnp.

References

Aguirre, J., Cachão, M., Domènech, R., Lozano-Francisco Ma, C., Martinell, J., Mayoral, E., Santos, A., Vera- Peláez, J.L., and Da Silva, C.M., 2005, Integrated biochronology of the Pliocene deposits of the Estepona basin (Málaga, S Spain). Palaeobiogeographic and palaeoceanographic implications: *Revista Española de Paleontología*, v. **20**, p. 225–244.

Albano, G.P., Hua, Q., Kaufman, D., and Zuschin, M., 2022, Young death assemblages with limited time-averaging in rocky and *Posidonia oceanica* habitats: *Geological Society, London, Special Publications*, v. **529**, https://doi.org/10.1144/SP529-2022-224.

Aspe, N.M., Cabales, R.G., Sajorne, R.E., and Creencia, L.A., 2019, Survey on the predators of abalone *Haliotis asinina* from the perspective of the local fisherfolks in selected sites of Palawan, the Philippines: *Journal of Shellfish Research*, v. **38**, p. 463–473.

Avila, S.P., Amen, R., Azevedo, J.M.N., Cachão, M., and Garcia-Talavera, F., 2002, Checklist of the Pleistocene marine molluscs of Praínha and Lagoínhas (Santa Maria Island, Azores): *Açoreana*, v. **9**, p. 343–370.

Bachry, S., Solihin, D.D., Gustiano, R., Soewardi, K., and Butet, N.A., 2019, Morphometric character and morphology of abalone *Haliotis squamata* Reeve 1864 in coastal southern Java and Bali: *Jurnal Ilmu dan Teknologi Kelautan Tropis*, v. **11**, p. 273–284.

Baluk, W., 1975, Lower Tortonian gastropods from Korytnica, Poland. Part I: *Palaeontologia Polonica*, v. **32**, 186 p.

Barnet, J.S.K., Harper, D.T., LeVay, L.J., Edgar, K.M., Henehan, M.J., *et al.*, 2020, Coupled evolution of temperature and carbonate chemistry during the Paleocene–Eocene; new trace element records from the low latitude Indian Ocean: *Earth and Planetary Science Letters*, v. **545**, n. 116414.

Bester-van der Merwe, A.E., D'Amato, M.E., Swart, B.L., and Roodt-Wilding, R., 2012, Molecular phylogeny of South African abalone, its origin and evolution as revealed by two genes: *Marine Biology Research*, v. **8**, p. 727–736.

Bial de Bellerade, C.P., 1903, *Haliotis neuvillii* nov. sp.: *Procès-Verbaux de la Société Linnéenne de Bordeaux, Bordeaux*, v. **58**, p. 196–198.

Bielecka, M., 1967, Trzeciorzęd poludniowo-zachodniej częsci Wyzyny Lubelskiej [The Tertiary of the south-western part of the Lublin Upland]: *Biuletyn Państwowego Instytutu Geologicznego*, v. **206**, p. 115–188.

Binkhorst, J.T., 1861, Monographie des Gasteropodes et des Cephalopodes de la Craie Superieure du Limbourg: Bruxelles, C. Muquardt, 83 p. [gastropods] + 44 p. [cephalopods].

Borghi, M., and Vecchi, G., 1998, La Malacofauna Plio-Pleistocenica del torrente Stirone (Pr). Haliotidae e Fissurellidae: *Parva Naturalia*, v. **5**, p. 77–04.

Bouchet, P., Rocroi, J-P., Hausdorf, B., Kaim, A., Kano, Y., Nützel, A., Parkhaev, P., Schrödl, M., and Strong, E.E., 2017, Revised classification, nomenclator and typification of gastropod and monoplacophoran families: *Malacologia*, v. **61**, 526 p.

Cavallo, O., and Repetto, G., 1992, Conchiglie fossili del Roero. Atlante Iconografico: *Associazione Naturalistica Piemontese, Memorie*, v. **2**, 253 p.

Cenni, F., Parisi, G., Scapini, F., and Gherardi, F., 2010, Sheltering behavior of the abalone, *Haliotis tuberculata* L., in artificial and natural seawater: the role of calcium: *Aquaculture*, v. **299**, p. 67–72.

Cherns, L., Wheeley, J.R., and Wright, V.P., 2011, Taphonomic Bias in Shelly Faunas Through Time: Early Aragonitic Dissolution and Its Implications for the Fossil Record, *in* Allison, P.A., and Bottjer, D.J., eds., *Taphonomy: Aims & Scope Topics in Geobiology Book Series*, v. 32: Dordrecht, Springer, https://doi.org/10.1007/978-90-481-8643-3_3.

Chiappa, G., Fassio, G., Corso, A., Crocetta, F., Modica, M.V., and Oliverio, M., 2022, How Many Abalone Species Live in the Mediterranean Sea?: *Diversity*, v. **14**, n. 1107, https://doi.org/10.3390/d14121107.

Chirli, C., 2004, Malacofauna Pliocenica Toscana, v. 4, Archaeogastropoda: Firenze, the author, Arti Grafiche BMB, 113 p.

Chirli, C., and Linse, U., 2011, The Pleistocene Marine Gastropods of Rhodes Island (Greece): Tavarnelle, the authors. 447 p.

Cossmann, A.É.M., 1896, Sur quelques formes nouvelles ou peu connues des faluns du Bordelais: *Association française pour l'Avancement des Sciences, Congrès de Bordeaux*, v. **2**, p. 442–452.

Cossmann, A.É.M., 1918, *Essai de Paléoconchologie comparée. 11 livraison*: Paris, chez l'Auteur, 388 p.

Cossmann, A.É.M., and Peyrot, A., 1917, Conchologie Néogénique de l'Aquitaine: *Actes de la Société Linnéenne de Bordeaux*, v. **69**, p. 157–365.

Cresti, M., and Forli, M., 2021, Intertidal rocky shore Gastropoda (Mollusca) from the Pliocene of Terre Rosse (Siena): *Bollettino Malacologico*, v. **57**, p. 192–202.

Crocetta, F., and Rismondo, S., 2009, *Haliotis mykonosensis* Owen, Hanavan and Hall, 2001 in the Procida Island (Gulf of Naples) and in the Central Mediterranean Sea, with notes on the Mediterranean Haliotidae: *Mediterranean Marine Science*, v. **10**, p. 139–144.

Csepreghy-Meznerics, I., 1954, Helvetische und tortonische Fauna aus dem östlichen Cserhátgebirge: *Annales de l'Institut Géologique de Hongrie*, v. **41**, 185 p.

Cunha, T.J., and Giribet, G., 2019, A congruent topology for deep gastropod relationships: *Proceedings of the Royal Society B, Biological Science*, v. **286**, n. 20182776.

Cunha, T.J., Reimer, J.D., and Giribet, G., 2021, Investigating sources of conflict in deep phylogenomics of vetigastropod snails: *Systematic Biology*, v. **71**, p. 1009–1022.

Davidaschvili, L.S., 1937, On the ecology of animals of the middle Miocene reefs of Ukrainian SSR: *Problems of Paleontology*, v. **2–3**, p. 537–563.

Davies, A.M., and Eames, F.M., 1971, *Tertiary Faunas, v.* 1: The Composition of Tertiary Faunas: New York, Elsevier, 571 p.

De Cristofori, G., and Jan, G., 1832, Cataloghi sistematici e descrittivi degli oggetti di storia naturale esistenti nel museo di Giuseppe De Cristofori e Prof. Giorgio Jan contenenti il Prodomo della Fauna, Della Flora e della Descrizione orittognostico-Geognostica dell'Italia Superiore: Milano, Coi Tipi di Giovanni Pirotta.

Delhaes, W., 1909, *Beitrage zur Morphologie und Phylogenie von Haliotis Linne*: Zeitschrift für induktive Abstammungs- und Vererbungslehre, v. **2**, p. 353–410.

Dominici, S., and Danise, S., 2023, Mediterranean onshore–offshore gradient in the composition and temporal turnover of benthic molluscs across the middle Piacenzian Warm Period, *in* Nawrot, R., Dominici, S., Tomašových, A., and Zuschin, M., eds., *Conservation Palaeobiology of Marine Ecosystems: Geological Society*, London, Special Publications, v. 529, https://doi.org/10.1144/SP529-2022-35.

Dominici, S., and Forli, M., 2021, Lower Pliocene molluscs from southern Tuscany (Italy): *Bollettino della Società Paleontologica Italiana*, v. **50**, p. 69–98, https://www.paleoitalia.it/bspi-vol-601/.

Dominici, S., Benvenuti, M., Forli, M., Bogi, C., and Guerrini, A., 2019, Upper Miocene molluscs of Monti Livornesi (Tuscany, Italy): biotic changes across environmental gradients: *Palaeogeography, Palaeoclimatology, Palaeoecology*, v. **527**, p. 103–117.

Dominici, S., Fornasiero, M.G., and Giusberti, L., 2020, The largest known cowrie and the iterative evolution of giant cypraeid gastropods: *Scientific Reports*, v. **10**, n. 21893.

Eichwald, C., 1829, Zoologia specialis quam expositis animalibus tum vivis, tum fossilibus potissimum Rossiae in universum, et Poloniae in specie, in usum lectionum publicarum in Universitate Caesarea Vilnensi. Pars prior: Vilnae, Typis Josephi Zawadzki.

Eichwald, E., 1853, *Lethaea rossica* ou Paléontologie de la Russie, décrite et figurée. Troisième volume. Dernière période: Stuttgart, Schweizerbart, 533 p.

Estes, J.A., Lindberg, D.R., and Wray, C., 2005, Evolution of large body size in abalones (*Haliotis*): *patterns and implications: Paleobiology*, v. **31**, p. 591–606.

Ferrero Mortara, E., Montefameglio, L., Pavia, G., and Tamperi, R., 1982, Catalogo dei tipi e degli esemplari figurati della collezione Bellardi and Sacco. Parte I: *Cataloghi Museo Regionale Scienze Naturali di Torino*, v. **6**, p. 3–327.

Ferrero Mortara, E., Montefameglio, L., Novelli, M., Opesso, G., Pavia, G., and Tamperi, R., 1984, Catalogo dei tipi e degli esemplari figurati della collezione Bellardi and Sacco. Parte II: *Cataloghi Museo Regionale Scienze Naturali di Torino*, v. **7**, p. 1–448.

Forli, M., Dell'Angelo, B., Ciappelli, F., and Taviani, M., 2003, A new species of Haliotidae (Mollusca: Vetigastropoda) in the Italian Pliocene: *Bollettino Malacologico*, v. **38**, p. 149–154.

Forli, M., Dell'Angelo, B., Montagna, P., and Taviani, M., 2004, A new large *Patella* (Mollusca: Patellogastropoda) in the Pliocene of the Mediterranean Basin: *Bollettino Malacologico*, v. **40**, p. 49–78.

Forli, M., Stalennuy, A., and Dell'Angelo, B., 2015, Reports of *Haliotis* Linnaeus, 1758 (Mollusca Vetigastropoda) from the middle Miocene of Ukraine: *Biodiversity Journal*, v. **6**, p. 87–94.

Forli, M., Cresti, M., and Corti, A., 2021, Further records of the family Patellidae Rafinesque, 1815 (Mollusca: Gastropoda) in the Tuscan Pliocene*: Bollettino Malacologico*, v. **57**, p. 152–163.

Friedberg, W., 1911–1928, *Mięczaki mioceńskie ziem Polskich. Cześć I. Ślimaki i Lódkonogi. (Mollusca Miocaenica Poloniae. Pars I. Gastropoda et Scaphopoda)*: Museum Imienia Dzieduszyckich, Lwów-Poznań, 631 p.

Geiger, D.L., 1998, Recent genera and species of the family Haliotidae Rafinesque, 1815 (Gastropoda: Vetigastropoda): *The Nautilus*, v. **111**, p. 85–116.

Geiger, D.L., 2000, Distribution and biogeography of the recent Haliotidae (Gastropoda: Vetigastropoda) world-wide: *Bollettino Malacologico*, v. **35**, p. 57–120.

Geiger, D.L., and Groves, L.T., 1999, Review of fossil abalone (Gastropoda: Vetigastropoda: Haliotidae) with comparison to Recent species: *Journal of Paleontology*, v. **73**, p. 872–885.

Geiger, D.L., and Owen, B., 2001, The identity of *Haliotis stomatiaeformis* Reeve, 1846, from the Mediterranean Sea: *The Nautilus*, v. **115**, p. 77–83.

Geiger, D.L., and Owen, B., 2012, Abalone: Worldwide Haliotidae: Hackenheim, Conchbooks, viii + 361 p.

Glibert, M., 1949, Gastropodes du Miocène moyen du Bassin de la Loire, 1: *Memoires de l'Institut Royal des Sciences Naturelles de Belgique*, v. **2**, 240 p.

Górka, M., Studencka, B., Jasionovski, M., Hara, U., Wysocka, A., and Poberezhskyy, A., 2012, The Medobory Hills (Ukraine): middle Miocene reef systems in the Paratethys, their biological diversity and lithofacies: *Biuletyn Państwowego Instytutu Geologicznego*, v. **449**, p. 147–174.

Grasso, M., and Pedley, H.M., 1988, The sedimentology and development of Terravecchia Formation carbonates (upper Miocene) of North Central Sicily: possible eustatic influence on facies development: *Sedimentary Geology*, v. **57**, p. 131–149.

Groves, L.T., and Alderson, M.J., 2008, Earliest record of the Genus *Haliotis* (Mollusca: Gastropoda) from the Late Cretaceous (Campanian) of Los Angeles County, California: *The Veliger*, v. **50**, p. 24–26.

Holland, S.M., and Christie, M., 2013, Changes in area of shallow siliciclastic marine habitat in response to sediment deposition: implications for onshore–offshore paleobiologic patterns: *Paleobiology*, v. **39**, p. 511–524.

Hörnes, M., 1851–1870, Die fossilen Mollusken des Tertiar-Beckens von Wien: *Abhandlungen der K. K. Geologischen Reichsanstalt*, v. **3**, p. 1–42 (1851), p. 43–208 (1852), p. 209–296 (1853), p. 297–383 (1854), p. 384–460 (1855), p. 461–736 (1856); v. 4, p. 1–479, (1870).

Invert E Base, 2023, All Collections, https://www.invertebase.org/portal/collections/list.php?taxa=120170&usethes=1&taxontype=2&page=1.

Inzani, A., 1983, Rinvenimento di esemplari di *Haliotis tubercolata lamellosoides* Sacco nel Pliocene della Val Chiavenna: *Notiziario Mineralogia e Paleontologia*, v. **36**, p. 12–15.

Itoigawa, J., and Tomida, S., 1982, *Miohaliotis amabilis*, a new haliotid fossil from the Miocene Mizunami Group, with special reference to fossil haliotid fauna in Neogene and Quaternary of Japan: *Bulletin of the Mizunami Fossil Museum. v. 9*, p. 1–14.

Jakubowski, G., and Musiał, T., 1979, Lithology and fauna of the middle Miocene deposits of Trzęsiny (Roztocze Tomaszowskie Region, South-eastern Poland): *Prace Muzeum Ziemi*, v. **32**, p. 37–70.

Jenkins, G.P., 2004, The ecosystem effects of abalone fishing: a review: *Marine and Freshwater Research*, v. **55**, p. 545–552.

Juárez-Ruiz, J., and Mas, G., 2022, Els dipòsits litorals atribuits històricament al Pliocè-Plistocè inferior de Mallorca (Illes Balears, Mediterrani occidental): revisió, biocronologia de molluscs i implicacions paleogeogràfiques: *Bolletí de la Societat d'Història Natural de les Balears*, v. **65**, p. 237–257.

Kaunhowen, F., 1897, Die Gastropoden der Maestrichter Kreide: *Palaeontologische Abhandlungen herausgegben von W. Dames und E. Koken, neue folge*, v. **4**, p. 3–126.

Kim, T.W., Lee, J.A., and Yoo, C.Y. 2020, Change of foraging and hiding behaviors in the Pacific abalone *Haliotis discus hannai* in response to elevated seawater temperature: *Ocean Science Journal*, v. **55**, p. 383–390.

Kiyomoto, S., Tagawa, M., Nakamura, Y., Horii, T., Watanabe, S., Tozawa, T., Yatsuya, K., Yoshimura, T., and Tamaki, A., 2013, Decrease of abalone resources with disappearance of macroalgal beds around the Ojika Islands, Nagasaki, Southwestern Japan: *Journal of Shellfish Research*, v. **32**, p. 51–58.

Kojumdgieva, E., and Strachimirov, B., 1960, Les fossilles de Bulgarie; VII, Tortonien: *Academie des Sciences de Bulgarie*, p. 1–246.

Korobkov, I. A., 1955, Spravochnik i metodicheskoe rukovodstvo po tretichnym molljuskam: *Brjuchonogie: Leningrad, Gostoptechizdat*, 795 p.

Krach, W., 1981, The Badeńskie utwory rafowe na Roztoczu Lubelskim [The Baden reef formations in Roztocze Lubelskie]: *Wydawnictwa Geologiczne*, v. **121**, p. 5–115.

Laghi, G.F., 1984, Sorprendente densità di *Chiton saeniensis* n. sp. in sabbie gialle plioceniche dei dintorni di Serre di Rapolano (Siena): *Bollettino del Museo Regionale di Scienze Naturali di Torino*, v. **2**, p. 555–564.

Lamarck, J.-B.M. de, 1822, *Histoire naturelle des animaux sans vertèbres, Tome sixième, 2me partie*: Paris, published by the author, 232 p.

Landau, B., Marquet, R., and Grigis M., 2003, The early Pliocene Gastropoda (Mollusca) of Estepona, southern Spain. Part 1: *Vetigastropoda: Palaeontos*, v. **3**, p. 1–87.

Landau, B.M., Van Dingenen, F., and Ceulemans, L., 2017, The upper Miocene gastropods of northwestern France, 1. Patellogastropoda and Vetigastropoda: *Cainozoic Research*, v. **17**, p. 75–166.

Lecointre, G., 1952, Recherches sur le Néogène et le Quaternaire marine de la côte Atlantique du Maroc: *Notes et Mémoires, Service Géologique du Maroc*, v. **99**, p. 1–173.

Li, J., Mao, Y., Jiang, Z., Zhang, J., Fang, J., and Bian, D., 2018, The detrimental effects of CO_2-driven chronic acidification on juvenile Pacific abalone (*Haliotis discus hannai*): *Hydrobiologia*, v. **809**, p. 297–308.

Linnaeus, C., 1758, *Systema naturæ per regna tria naturæ, secundum classes, ordines, genera, species, cum characteribus, differentiis, synonymis, locis, v. 1 (tenth edition), Revised*: Stockholm, Salvius, 824 p.

Lozano-Francisco, M., and Vera-Peláez, J.L., 2002, Estudio preliminary del orden Archaegastropoda (Gastropoda, Prosobranchia) del Plioceno de la Cuenca de Estepona (Máalaga, S España) con la description de doce especies nuevas: *Pliocénica*, v. **2**, p. 157–175.

Lozouet, P., Maestrati, P., Dolin, L., and Favia, R., 2001a, Un site exceptionnel du Miocène inférieur (Aquitanien): la "Carrière Vives" (Meilhan, Landes, France). Bilan de la campagne de fouilles de juillet - août 1991: *Cossmanniana*, v. **8**, p. 47–67.

Lozouet, P., Lesport, J-F., and Renard, P.H., 2001b, Révision des Gastropoda (Mollusca) du Stratotype de l'Aquitanien (Miocène Inf.): site de Saucats "Laryei", Gironde, France: *Cossmanniana, Hors sèrie*, v. **3**, p. 1–189.

Lundgren, B., 1894, Jamforelse mellan Molluskfaunan i Mammillatus och Mucronata Zonera I Nordostra Skane (Kruistianstadsomradet): *Kongl Svenska Veteskaps-Akademiens Handlingar*, v. **26**, p. 3–58.

Mandic, O., and Steininger, F.F., 2003, Computer-based mollusc stratigraphy—a case study from the Eggenburgian (lower Miocene) type region (NE Austria): *Palaeogeography, Palaeoclimatology, Palaeoecology*, v. **197**, p. 263–291, https://doi.org/10.1016/S0031-0182(03)00469-3.

Martini, I., and Aldinucci, M., 2017, Sedimentation and basin-fill history of the Pliocene succession exposed in the northern Siena–Radicofani Basin (Tuscany, Italy): a sequence stratigraphic approach: *Rivista Italiana di*

https://doi.org/10.1017/jpa.2024.50 Published online by Cambridge University Press

Paleontologia e Stratigrafia, v. **23**, p. 407–432, https://doi.org/10.13130/2039-4942/9017.

McShane, P.E., Schiel, D.R., Mercer, S.F., and Murray, T., 1994, Morphometric variation in *Haliotis iris* (Mollusca:Gastropoda): analysis of 61 populations: *New Zealand Journal of Marine and Freshwater Research*, v. **28**, p. 357–364.

Mgaya, Y.D., and Mercer, J.P., 1994, A review of the biology, ecology, fisheries and mariculture of the European abalone *Haliotis tuberculata* Linnaeus 1758 (Gastropoda: Haliotidae): Biology and Environment: *Proceedings of the Royal Irish Academy*, v. **94B**, p. 285–304.

Michelotti, G., 1847, Description des fossiles des terrains Miocènes de l'Italie septentrionale : *Natuurkundige Verhandelingen van de Hollandsche Maatschappij der Wetenschappen te Haarlem*, v. **3**, p. 1–409.

Mondanaro, A., Dominici, S., and Danise, S., 2024, Response of Mediterranean Sea bivalves to Pliocene–Pleistocene environmental changes: *Palaeontology*, v. **2024**, n. e12696.

Monfort, P., 1810, *Conchyliologie systématique et classification méthodique des coquilles, v. 2*: Paris, Schoell, 676 p.

Nalin, R., Ghinassi, M., Foresi, L., and Dallanave, E., 2016, Carbonate deposition in restricted basins: a Pliocene case study from the central Mediterranean (northwestern Apennines): *Journal of Sedimentary Research*, v. **86**, p. 236–267.

Neuman, M., Tissot, B., and Vanblaricom, G., 2010, Overall status and threats assessment of Black Abalone (*Haliotis Cracherodii* Leach, 1814) populations in California: *Journal of Shellfish Research*, v. **29**, p. 577–586.

Oksanen, J., Simpson, G., Blanchet, F., Kindt, R., Legendre, P., *et al.*, 2022, vegan: Community Ecology Package. R package version 2.6-4, https://cran.r-project.org/web/packages/vegan/vegan.pdf (accessed Aug 2024).

Owen, B., 2003, The buzz on abalones. The neglected *Haliotis*: *Haliotis stomatiaeformis* Reeve, 1846: *Of Sea and Shore*, v. **25**, p. 286–289.

Owen, B., 2006, The correct identity of the type lot of *Haliotis speciosa* Reeve, 1846 and proposed appropriate nomenclatural changes that reflect this discovery: *Of Sea and Shore*, v. **27**, p. 204–207, 209–210, 213–214.

Owen, B., 2013, Notes on the correct taxonomic status of *Haliotis rugosa* Lamarck, 1822, and *Haliotis pustulata* Reeve, 1846, with description of a new subspecies from Rodrigues Island, Mascarene Islands, Indian Ocean (Mollusca: *Vetigastropoda: Haliotidae): Zootaxa*, v. **3646**, p. 189–193.

Owen, B., 2014, A new species of *Haliotis* (Gastropoda) from São Tomé & Príncipe Islands, Gulf of Guinea, with comparisons to other *Haliotis* found in the Eastern Atlantic and Mediterranean: *Zootaxa*, v. **3838**, p. 113–119.

Owen, B., and Afonso C.M.L., 2012, A new subspecies of *Haliotis tuberculata* Linnaeus, 1758 from Cape Verde Island, Central West Africa. Addendum 2: *in* Geiger, D.L., and Owen, B., eds., Abalone: Worldwide Haliotidae: Hackenheim, Conchbooks, viii + 361 p.

Owen, B., and Berschauer, D., 2017, An iconography of *Haliotis volhynica* Eichwald, 1829, and description of a new species of *Haliotis* from the middle Miocene of Ukraine: *The Festivus*, v. **49**, p. 39–44.

Owen, B., Hanavan, S., and Hall, S., 2001, A new species of abalone (*Haliotis*) from Greece: *The Veliger*, v. **44**, p. 301–309.

Owen, B., Ryall, P., and Pan, A.D., 2015, Iconography and distribution of the Cape Verde Island Abalone, *Haliotis tuberculata fernandesi* Owen & Afonso, 2012, with comparisons to *H. tuberculata coccinea* Reeve, 1846, of the Canary Islands: *The Festivus*, v. **47**, p. 243–249.

Peters, H., 2021, *Haliotis tuberculata*. The IUCN Red List of Threatened Species 2021: *e.T78772221A78772628*, https://dx.doi.org/10.2305/IUCN.UK.2021-3.RLTS.T78772221A78772628.en (accessed Sep 2023).

Philippi, R.A., 1848, Testaceorum novorum centuria: *Zeitschrift für Malakozoologie*, v. **5**, p. 13–16.

Ponder, W.F., and Lindberg, D.R., 2008, *Phylogeny and Evolution of the Mollusca (first edition)*: Berkeley, University of California Press, 900 p.

Radwański, A., Górka, M., and Wysocka, A., 2006, Middle Miocene coralgal facies at Maksymivka near Ternopil (Ukraine): a preliminary account: *Acta Geologica Polonica*, v. **56**, p. 89–103.

Rafinesque, C.S., 1815, *Analyse de la nature ou Tableau de l'univers et des corps organisés*: Palermo, Rafinesque, 224 p.

R Core Team, 2022, *R: A Language and Environment for Statistical Computing*: Vienna, R Foundation for Statistical Computing.

Reeve, L.A., 1846, *Conchologia Iconica: or, Illustrations of the Shells of Molluscous Animals*, v. **3**: London, Reeve Brothers, 237 p.

Reitano, A., Di Franco, D., and Scuderi, D. 2024, Further new taxonomical and paleontological notes on *Haliotis stomatiaeformis* Reeve, 1846 (Gastropoda Haliotidae): *Biodiversity Journal*, v. **15**, p. 319–326.

Rogers-Bennett, L., and Catton, C.A., 2019, Marine heat wave and multiple stressors tip bull kelp forest to sea urchin barrens: *Scientific Reports*, v. **9**, n. 15050.

Rogers-Bennet, L., Haaker, P.L., Huff, T.O., and Dayton, P.K., 2002, Estimating baseline abundances of abalone in California for restoration: California Cooperative Oceanic Fisheries Investigations Report 43, p. 97–111.

Roussel, V., and Van Wormhoudt, A., 2017, The effect of Pleistocene climate fluctuations on distribution of European abalone (*Haliotis tuberculata*), revealed by combined mitochondrial and nuclear marker analyses: *Biochemical Genetics*, v. **55**, p. 124–154.

Ruggieri, G., 1990, Una *Haliotis* del Miocene superiore (Saheliano) della Sicilia: *Bollettino Malacologico*, v. **25**, p. 349–354.

Sacco, F., 1897, *I Molluschi dei terreni terziari del Piemonte e della Liguria. Parte XXII. Gasteropoda, (fine), Amphineura, Scaphopoda*: Torino, Carlo Clausen, 149 p.

Saint Martin, J.-P., Merle, D., Cornée, J.-J., Filipescu, L., Saint Martin, S.S., and Bucur, I.I., 2007, The Badenian (middle Miocene) coral build-ups of the western border of the Transylvanian Basin (Romania): *Comptes Rendus PaleVol*, v. **6**, p. 37–46.

Searcy-Bernal, R., and Gorrostieta-Hurtado, E., 2007, Effect of darkness and water flow rate on survival, grazing and growth rates of abalone *Haliotis rufescens* postlarvae: *Journal of Shellfish Research*, v. **26**, p. 789–794.

Sessa, J.A., Callapez, P.M., Dinis, P.A., and Hendy, A.J.W., 2013, Paleoenvironmental and paleobiogeographical implications of a Middle Pleistocene mollusc assemblage from the marine terraces of Baía Das Pipas, southwest Angola: *Journal of Paleontology*, v. **87**, p. 1016–1040.

Śliwiński, M., Bąbel, M., Nejbert, K., Olszewska-Nejbert, D., Gąsiewicz, A., Schreiber, B.C., Benowitz, J.A., and Layer, P., 2012, Badenian–Sarmatian chronostratigraphy in the Polish Carpathian Foredeep: *Palaeogeography, Palaeoclimatology, Palaeoecology*, v. **326–328**, p. 12–29.

Sohl, N.F., 1992, Upper Cretaceous gastropods (Fissurellidae, Haliotidae, Scissurellidae) from Puerto Rico and Jamaica: *Journal of Paleontology*, v. **66**, p. 414–434.

Southgate, P.C., and Militz, T.A., 2023, A multivariate approach to morphological study of shell form in cowries (Gastropoda, Cypraeidae): a case study with *Umbilia armeniaca* (Verco, 1912): *ZooKeys*, v. **1158**, p. 69–89.

Steininger, F., 1963, Die Molluskenfauna aus dem Burdigal (unter-Miozän) von Fels am Wagram in Niederösterreich: *Denkschriften, Österreichische Akademie der Wissenschaften, Mathematisch-Naturwissenschaftliche Klasse*, v. **110**, p. 1–88.

Strausz, L., 1966, *Die Miozän-Mediterranen Gastropoden Ungarns*: Budapest, Akadémiai Kiadó, 693 p.

Swainson, W., 1822, *Zoological Illustrations, or, Original Figures and Descriptions of New, Rare, or Interesting Animals, Selected Chiefly from the Classes of Ornithology, Entomology, and Conchology, and Arranged on the Principles of Cuvier and Other Modern Zoologists, v. 2*: London, Baldwin, Cradock and Joy; and W. Wood.

Talmadge, R.R., 1971, Notes on Israeli *Haliotis* (Mollusca, Gasteropoda): *Argamon*, v. **2**, p. 81–85.

Tomida, S., Okumura, Y., and Kaede, T., 2006, A mature specimen of *Haliotis amabilis* (Itoigawa and Tomida, 1982), from middle Miocene of central Japan, and its paleontological significance: *Bulletin of the Mizunami Fossil Museum*, v. **33**, p. 111–114.

Uribe, J.E., Makiri, S., and Harasewych, M.G., 2022, The mitogenome of the sunken wood limpet *Notocrater youngi*: insights into mitogenome evolution in Lepetellida (Gastropoda: Vetigastropoda): *Journal of Molluscan Studies*, v. **88**, n. eyac009.

Van Wormhoudt, A., Le Bras, Y., and Huscette, S., 2009, *Haliotis marmorata* from Senegal; a sister species of *Haliotis tuberculata*: morphological and molecular evidence: *Biochemical Systematics and Ecology*, v. **37**, p. 747–755.

Van Wormhoudt, A., Gaume, B., Le Bras, Y., Roussel, V., and Huchette, S., 2011, Two different and functional nuclear rDNA genes in the abalone *Haliotis tuberculata*: tissue differential expression: Genetica, v. 139, p. 1217–1227.

Vera-Peláez, J.L., and Lozano-Francisco, M.C., 2022, Réplica a "Additions and corrections to the gastropod fauna of the Pliocene of Estepona,

https://doi.org/10.1017/jpa.2024.50 Published online by Cambridge University Press

south-western Spain 4" Landau, B.M. & Mulder, H. Basteria 84(1–3) 2020 y "The Early Pliocene Gastropoda (Mollusca) from Estepona (souther Spain), Part 1: *Vetigastropoda" Landau, B.M., Marquet, R. & Grigis, M. Palaeontos, 2003: Pliocénica*, v. **6–7**, p. 1–51.

Wells, F.E., Keesing, J.K., Gagnon, M.M., Bessey, C., Spilsbury, F., and Irvine, T.R., 2023, Responses of intertidal invertebrates to rising sea surface temperatures in the southeastern Indian Ocean: *Frontiers in Marine Science*, v. **10**, n. 1075228.

WoRMS, 2023, Gastropoda, http://www.marinespecies.org/aphia.php?p=taxdetails&id=101 (accessed Aug 2023).

Yasuhara, M., Huang, H.-H.M., Reuter, M., Tian, S.Y., Cybulski, J.D., *et al.*, 2022, Hotspots of Cenozoic tropical marine biodiversity: *Oceanography and Marine Biology: An Annual Review*, v. **60**, p. 243–300.

Zelinskaya, V.A., Kulichenko, V.G., Makarenki, D.E., and Sorochan, E.A., 1968, Gastropod and scaphopod mollusks of the Paleogene and Miocene of the Ukraine: *Paleontologiceskij Spravocnik*, v. **2**, p. 1–282.

Zenetos, A., Gofas, S., Russo, G., and Templado, J., 2004, Molluscs: *CIESM Atlas of Exotic Species in the Mediterranean*, v. **3**, 378 p.

Zunino, M., and Pavia, G., 2009, Lower to middle Miocene mollusc assemblages from the Torino Hills (NW Italy): *synthesis of new data and chronostratigraphical arrangement: Rivista Italiana di Paleontologia e Stratigrafia*, v. **115**, p. 349–370.

Zuschin, M., Stachowitsch, M., and Stanton, R.J., Jr., 2003, Patterns and processes of shell fragmentation in modern and ancient marine environments: *Earth-Science Reviews*, v. **63**, p. 33–82.

https://doi.org/10.1017/jpa.2024.50 Published online by Cambridge University Press